Journal of Contaminant Hydrology 210 (2018) 15–30

Contents lists available at ScienceDirect

Journal of Contaminant Hydrology

journal homepage: www.elsevier.com/locate/jconhyd

Monitoring well utility in a heterogeneous DNAPL source zone area: Insights from proximal multilevel sampler wells and sampling capture-zone modelling

Lindsay A. McMillan[a,b,*], Michael O. Rivett[c,d,**], Gary P. Wealthall[e], Peter Zeeb[f], Peter Dumble[g]

[a] School of Geography Earth and Environmental Sciences, University of Birmingham, Birmingham B15 2TT, UK
[b] Mott MacDonald, 2 Brewery Wharf, Kendall St, Leeds LS10 1JR, UK
[c] GroundH$_2$O Plus Ltd, Quinton, Birmingham B32 1DY, UK
[d] Department of Civil and Environmental Engineering, University of Strathclyde, Glasgow G1 1XJ, UK
[e] Geosyntec Consultants, Inc., 130 Stone Road West, Guelph, Ontario N1G 3Z2, Canada
[f] Geosyntec Consultants, Inc., 289 Great Road, Suite 202, Acton, MA 01720, USA
[g] Peter Dumble Hydrogeology, Tiverton, Devon EX16 7TA, UK

ARTICLE INFO

Keywords:
Groundwater sampling
Monitoring wells
Groundwater quality
Low-flow sampling
DNAPL
Flow-weighted average (FWA) concentration

ABSTRACT

Groundwater-quality assessment at contaminated sites often involves the use of short-screen (1.5 to 3 m) monitoring wells. However, even over these intervals considerable variation may occur in contaminant concentrations in groundwater adjacent to the well screen. This is especially true in heterogeneous dense non-aqueous phase liquid (DNAPL) source zones, where cm-scale contamination variability may call into question the effectiveness of monitoring wells to deliver representative data. The utility of monitoring wells in such settings is evaluated by reference to high-resolution multilevel sampler (MLS) wells located proximally to short-screen wells, together with sampling capture-zone modelling to explore controls upon well sample provenance and sensitivity to monitoring protocols. Field data are analysed from the highly instrumented SABRE research site that contained an old trichloroethene source zone within a shallow alluvial aquifer at a UK industrial facility. With increased purging, monitoring-well samples tend to a flow-weighted average concentration but may exhibit sensitivity to the implemented protocol and degree of purging. Formation heterogeneity adjacent to the well-screen particularly, alongside pump-intake position and water level, influence this sensitivity. Purging of low volumes is vulnerable to poor reproducibility arising from concentration variability predicted over the initial 1 to 2 screen volumes purged. Marked heterogeneity may also result in limited long-term sample concentration stabilization. Development of bespoke monitoring protocols, that consider screen volumes purged, alongside water-quality indicator parameter stabilization, is recommended to validate and reduce uncertainty when interpreting monitoring-well data within source zone areas. Generalised recommendations on monitoring well based protocols are also developed. A key monitoring well utility is their proportionately greater sample draw from permeable horizons constituting a significant contaminant flux pathway and hence representative fraction of source mass flux. Acquisition of complementary, high-resolution, site monitoring data, however, vitally underpins optimal interpretation of monitoring-well datasets and appropriate advancement of a site conceptual model and remedial implementation.

1. Introduction

Monitoring wells have been used extensively worldwide for the assessment of groundwater quality at contaminated sites (Barber and Davis, 1987; Basu et al., 2006; FDEP, 2008; Fretwell et al., 2006; Puls and Paul, 1997). Even though most wells nowadays are screened over relatively short intervals of 1.5 to 3 m (5 to 10 ft), the variation in groundwater quality within the screen-adjacent geological formation over even these length scales may still be considerable. At dense non-aqueous phase liquid (DNAPL) contaminated sites, orders of magnitude changes in dissolved-phase concentrations may occur locally in source-zone areas arising from the marked spatial variability in the occurrence of residual DNAPL contributing to dissolved-phase plume contaminaion (Guilbeault et al., 2005; Johnston et al., 2013; Parker et al., 2003;

* Correspondence to: Lindsay A. McMillan, Mott MacDonald, 2 Brewery Wharf, Kendall St, Leeds LS10 1JR, UK.
** Correspondence to: Michael O. Rivett, GroundH$_2$O Plus Ltd, Quinton, Birmingham B32 1DY, UK.
E-mail addresses: Lindsay.Mcmillan@mottmac.com (L.A. McMillan), rivett@groundh2oplus.co.uk (M.O. Rivett).

https://doi.org/10.1016/j.jconhyd.2018.02.001
Received 22 November 2017; Received in revised form 26 January 2018; Accepted 2 February 2018
Available online 09 February 2018

Rivett and Feenstra, 2005). Resolution of this variability may be required to better understand where the principal fluxes of contamination originate from. Also, where to surgically target remediation efforts to address discretely layered persistent DNAPL and diffused, secondary source zone, mass within low-permeability units increasingly characteristic in later stages of source zone aging (Kueper et al., 2014; Rivett et al., 2014).

Justifiably, the utility of monitoring wells, even short-screen, to deliver data appropriate to develop such surgical efforts may be called into question. Although monitoring wells will typically detect the presence of a DNAPL source area via the observation of elevated concentrations relative to the wider site, pumped groundwater samples will provide an averaged concentration drawn from across the well-screen length. Theoretically under a steady-state flow condition, a pumped sample should provide a flow-weighted average (FWA) concentration, i.e., an average of the formation's vertical heterogeneous concentration distribution weighted by the vertical distribution of flow rates, or formation hydraulic conductivities (K) in a flow system characterised by horizontal gradients (Martin-Hayden and Britt, 2006; McMillan et al., 2014; Puls and Barcelona, 1996). A wide spectrum of methods has become available to sample monitoring wells with potential to deliver a FWA concentration (Britt et al., 2010; ITRC, 2007; McHugh et al., 2016; Parsons, 2005; Puls and Barcelona, 1996; US EPA, 2010, 2013, 2017; Vroblesky, 2001). These may be categorized under:

- 'Zero/minimal-purge' protocols using grab or passive diffusion-based samplers that remove none or a very small water volume prior to sampling, and effectively obtain a grab sample of the ambient flow regime occurring at the point or interval monitored within the well screen.
- 'Low-flow' (low stress) protocols that purge and sample at low flow rates until indicator parameter stabilization occurs, and may involve low to moderate volumes of water being extracted to achieve this condition.
- 'Multiple well-volume purging' (fixed volume purge) protocols that are based upon a specified number of well volumes being purged prior to sampling.

Our focus is upon pumped samples and hence low-flow and multiple well-volume purging protocols, but cognizant of the fact that the ambient conditions existent within the well-screen that control a zero/minimal-purge protocol sample provenance also constitute the initial condition to, and remain influential during, purging progressed under the studied protocols. The in-well ambient condition is perhaps surprisingly complex and can be difficult to predict a priori. Whilst natural gradient through-flow across the well screen fundamentally occurs, with cross-well lateral flushing rates controlled by the formation K profile (Robin and Gillham, 1987), the in-well stratified contamination resulting may be variously perturbed. Formation vertical hydraulic gradients may induce up/downward in-well flows. In-well mixing (redistribution) may also arise from convection due to temperature gradients and fluid density effects, lateral or vertical flow turbulence and contaminant diffusion gradients (Martin-Hayden and Britt, 2006; McMillan et al., 2014; ITRC, 2006, 2007; Vroblesky et al., 2006). A FWA concentration may only arise for a zero/minimal-purge sample if full mixing of just groundwater flowing through the screen section occurs. More probable is that heterogeneous groundwater concentrations entering the well are irregularly and incompletely mixed alongside possible mixing with blank casing water that is susceptible to convection (Martin-Hayden and Britt, 2006). The more recent work of Britt et al. (2014) concludes that whilst most wells are expected to experience significant redistribution effects, some wells may maintain stratification or potentially even re-stratify differently from the surrounding formation.

Under both low-flow and multiple well volume purging protocols, provided that a steady state flow condition is reached, then a FWA concentration is expected (Varljen et al., 2006). Whether purge times (and hence purged volumes) are adequate to attain a steady-state FWA sample concentration, however, is a key issue (Martin-Hayden, 2000; Martin-Hayden et al., 2014; McMillan et al., 2014). The variation in delayed arrival times within the sample taken of groundwater entering the monitoring well screen at distance from the pump intake becomes of critical significance here (Martin-Hayden et al., 2014). Where protocols are based upon a specified number of (standing water) well or screen volumes purged prior to sampling, then greater volumes increase the likelihood of a steady-state FWA sample being obtained. For low-flow (low-stress) sampling protocols, where steady-state conditions are evidenced by stabilization of the pumping water level and water quality indicator parameters (EC, pH, etc.) (Puls and Barcelona, 1996; US EPA, 2010, 2017), these protocols typically do not indicate a minimum purged volume (other than to specify it exceeds any well drawdown measured and sample equipment volume). Where comparatively low volumes are purged, then a partial (rather than full) purge of the original standing well (or screen) water volume will occur (Martin-Hayden et al., 2014) and samples may then be expected to variously approach, but not fully constitute, a FWA sample concentration. It is clear from the above that understanding the influence of employed protocols upon monitoring well assessment of heterogeneous DNAPL source zone areas is of critical importance.

Whilst higher resolution site assessment alternative technologies have become increasingly recommended (Anneser et al., 2008; Basu et al., 2009; Kram et al., 2001; ITRC, 2015), their use is still perceived to represent a small fraction of the site characterization effort worldwide that still predominantly involves monitoring wells. Alternatives to characterize source-zone mass distribution include, detailed core sampling (Parker et al., 2003), inter-well partitioning tracer tests (Annable et al., 1998) and direct-push methods involving direct water sampling ("groundwater profiling") and indirect measurements using sensor-based tools such as the Membrane Interface Probe (Adamson et al., 2014; Guilbeault et al., 2005). Alternatives to resolve dissolved-phase plume mass fluxes include, multi-level sampler (MLS) transect monitoring (Basu et al., 2006; Béland-Pelletier et al., 2011; Johnston et al., 2013) as well as those extending monitoring well (or long-screen borehole) utility such as Passive Flux Meter (Annable et al., 2005), Integral Pumping Test (Béland-Pelletier et al., 2011), or Flexible Membrane Liner approaches (Cherry et al., 2007). Such alternatives, despite their benefits, can still be perceived as onerous. MLS transect monitoring, for instance, may be viewed not cost-effective due to the sheer numbers of MLS point samples involved and the large resource allocated to a small, albeit important, locality within the much larger site. This view is perhaps reasonable when it is recognised that even research-based studies (Cai et al., 2012; King et al., 1999; Kao and Wang, 2001; Einarson and Mackay, 2001) may fail to achieve MLS transect minimum sample densities necessary to estimate mass discharge with quantified uncertainty (Brooks et al., 2015; Li et al., 2007).

It is concluded that the continued use of monitoring wells to characterize source zones is not because they are technically more effective than alternative assessment options. Typically, they are not expected to be; but rather, they offer a cost-effective, easily implemented and widely accepted approach to site assessment that can be implemented from the detailed source zone to greater site scales to give an integrated, but reasonable indication, of contamination present. Recognizing the conundrum that monitoring well use is hence non-ideal, but set to continue into the foreseeable future, it remains imperative that monitoring wells are not simply used as an unthinking default option. Rather, we seek to better understand and improve upon their utility, including their collaborative use with the aforementioned higher resolution alternatives alongside considered interpretation. This ambition provides critical impetus to the research herein. Surprisingly few site studies have evaluated the detailed origin of groundwater sampled by monitoring wells despite their near-ubiquitous use. Available studies, whilst offering explanations for sample provenance

(Hutchins and Acree, 2000; McDonald and Smith, 2009; Metcalf and Robbins, 2007; Puls and Paul, 1997; Reilly and LeBlanc, 1998; Sukop, 2000), typically lack the ideal of detailed corroborating data. This notably includes data afforded by proximal high-resolution MLS transects that could be used to estimate groundwater flows and concentrations contributing to a well sample from the horizons screened. Furthermore, the above studies have often focused upon monitoring wells (boreholes) with screen lengths over 3 m, sometimes considerably so.

Our field-based research has been conducted at the SABRE (Source Area BioREmediation) site located in the UK where a trichloroethene (TCE) DNAPL source area has been intensively monitored prior to and throughout a pilot-scale bioremediation field trial (Buss et al., 2010). The historic industrial spill site provided a unique field-scale opportunity to compare traditional monitoring well sampling with proximal MLS transect data and develop insight to the provenance of monitoring well samples within an aged DNAPL source zone set within a typically heterogeneous sand-gravel aquifer. The goal was to use field-scale evidence gained from conventional monitoring well and proximal MLS sampling, together with supporting numerical model simulation of monitoring well capture zones, to better understand the provenance of samples obtained during conventional sampling focusing on low-flow and multiple well-volume purging of typical short-screen monitoring wells. Objectives were: to evaluate proximal MLS – monitoring well data within the existing SABRE research study field dataset obtained during baseline monitoring and bioremediation phases; to use numerical flow and transport modelling to inform the field-scale study interpretation and to explore sensitivities to monitoring well sample origins and sampling protocols; and, to consider the implications of sampling scale and well screen length for practitioners regarding the utility of monitoring wells, particularly within DNAPL source zone areas.

2. Materials and methods

2.1. Field site and historical field data overview

Specific data relevant to our project aim were drawn from the larger dataset of the SABRE project concerning the in-situ bioremediation of an aged TCE-DNAPL source zone (Buss et al., 2010; Dearden et al., 2010a; Harkness et al., 2012; Robinson et al., 2009; Wilson and Cai, 2010; Zeeb and Houlden, 2010). The source area contamination is the result of TCE releases from subsurface effluent pipes at a chemical manufacturing plant in the UK Midlands over a plant operational period spanning 20 to 45 years prior to the SABRE study. The source-zone architecture has been shown in detail to be spatially heterogeneous (Rivett et al., 2014).

The shallow aquifer underlying the site consists of *c.* 1 m of made ground overlying *c.* 5 m of superficial Quaternary alluvium and river terrace gravels (Chambers et al., 2010; Dearden et al., 2013). Below this lies *c.* 50 m of relatively impermeable Triassic mudstone (Mercia Mudstone Group) which may be weathered in the top 0.5 to 1.25 m (Chambers et al., 2010). The Quaternary deposits are heterogeneous; they are generally finer in the upper *c.* 1–2 m and comprise a sequence of alluvial sands, silts and clays with mm scale laminations (Lelliot et al., 2008; Chambers et al., 2010). These finer deposits grade into *c.* 4 m of poorly sorted river terrace deposits. The river terrace deposits comprise coarser sands and gravels formed from river channel deposition. The water table is typically 1–2 m bgl (below ground level) with hydraulic gradients of 0.001–0.002 towards a local river (Chambers et al., 2010; Dearden et al., 2013).

A key feature of the SABRE project of advantage to our study was the constrained known groundwater flow regime afforded by the installation of the 3-sided U-shaped SABRE test cell comprising sealed plastic sheet pile walls keyed into the underlying mudstone aquitard (Fig. 1). The cell was oriented parallel to the prevailing groundwater flow direction and isolated a portion of the DNAPL source zone around 3–13 m along the cell length (Buss et al., 2010; Rivett et al., 2014). The cell is open upgradient of the source zone to allow groundwater inflow with an abstraction well positioned at the closed cell end that controlled groundwater flow rates, and residence time, along the length of the cell streamtube created. The well abstraction rate during cell operation of 1.4–1.6 l/min was chosen to give groundwater velocities of 0.7 m/d (comparable to the natural) and a nominal cell residence time of around 42 days (Cai et al., 2012; Rivett et al., 2014). Cell water levels, as measured at SW70 and SW75 monitoring wells (and T2a and T3a transects) (Fig. 1), were variable during cell operation; typically values were 2–4 m bgl with decreasing water levels ascribed to partial cell dewatering from clogging at the entrance reducing cell inflow rates part way through the study (then overcome by additional groundwater pumping into the cell).

We draw upon data from the seven detailed sampling operations (Table 1) conducted during the 2-year operational period (Buss et al., 2010). The initial three sampling operations (Op. 1 to Op. 3) were during the baseline (pre-bioremediation) period and the remaining four during the bioremediation phase (Op. 4 to Op. 7) involving electron donor injection and bioaugmentation (Harkness and Fisher, 2013; Cai et al., 2012). Increased occurrence of TCE dechlorination products, cDCE (cis-dichloroethene), VC (vinyl chloride *aka.* chloroethene) and ETH (ethene) was found during this later phase (Wilson and Cai, 2010).

High-resolution groundwater monitoring was undertaken in the source zone and in the down-gradient dissolved-phase plume using MLS transects installed both perpendicular to and parallel with groundwater flow. In addition to the MLS transects, a number of 3-m screen, 50 mm diameter monitoring wells were installed. Two such monitoring wells and their adjoining MLS transects comprise the focus of this study: monitoring well SW70 positioned close to the down-gradient boundary of the DNAPL source zone and monitoring well SW75 within the dissolved plume, down-gradient of the source (Fig. 1). MLS transects T2a and T3a provided very proximal depth-discrete contaminant concentration distribution data from their positions immediately upgradient of SW70 and SW75 respectively. These transects each contained seven MLSs that were spaced equally across the cell at 0.5 m intervals. Each MLS comprised a bundle of nine HDPE 10 mm (internal diameter) sampling tubes completed at different depths. The lowermost 15-cm interval of each tube was slotted and over-wrapped in geotextile to serve as a discrete sampling port. MLS ports were spaced at 0.5 m intervals vertically and installed to monitor the 4-m thick superficial aquifer immediately overlying the mudstone (Fig. 1). A total of 63 ports within each transect spaced 0.5 m laterally and vertically hence allowed detailed spatial characterization of contaminant concentrations in the cell passing SW70 and SW75 well screens that were centrally positioned (laterally and vertically) with respect to their associated MLS transect *c.* 1 m up-gradient.

SW70 and SW75 were sampled using a 12 V submersible pump (WaSP®) positioned just within the lower 1 m interval of the well-screen interval. Pumping was undertaken at rates of 1–5 l/min with the motivation that traditional purged monitoring well water quality samples would result. Purged water was monitored for stabilization of water quality parameters with removal of a minimum of 3 well volumes (24 l, assuming typical rest water levels at 2 m bgl) prior to taking samples for VOC (volatile organic compound) and supporting hydrochemical analysis. Similar to Martin-Hayden et al. (2014), we later report and simulate time-variant data as screen volumes (SV) removed (purged) as opposed to well volumes. For a 3 m × 50 mm diameter well screen, 3 SV is equivalent to 18 l. With minimal drawdown sampling where the pump intake is located within the well screen, little sample water is expected to originate from the blank-casing. Also, the screen volume is fixed across different sampling events as long as drawdown remains above the top of the well screen.

T2a and T3a MLS transects were sampled at 200 ml/min using a peristaltic pump. Transect port samples within 10 mm diameter tubes were taken following chemical stabilization with a minimum of 3

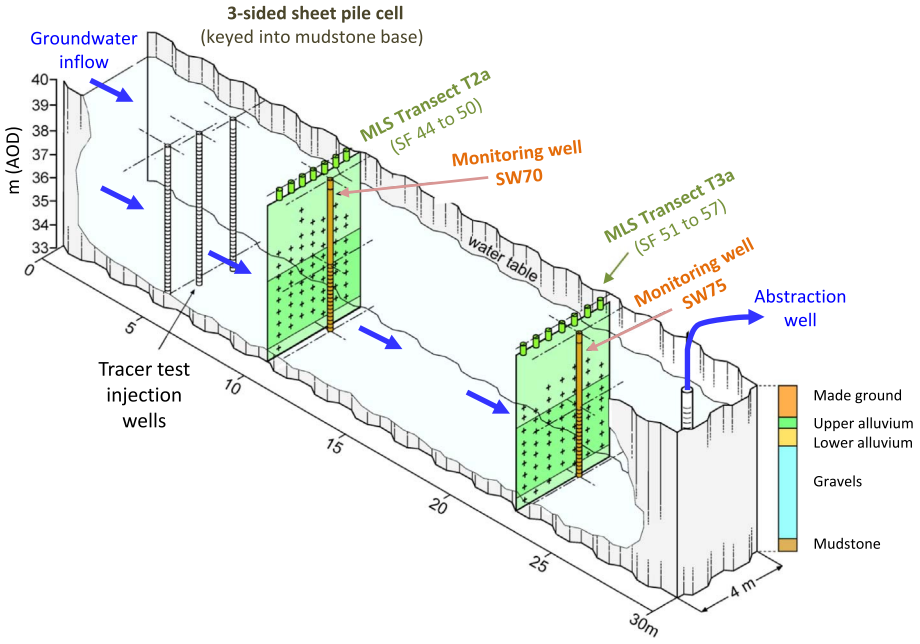

Fig. 1. Schematic of SABRE test cell illustrating the monitoring infrastructure used in the present study.

Table 1
SABRE Sampling Operations (Op.) relative to the start of the bioremediation phase at Day 0: negative days cover the baseline period and positive days the active remediation phase. Cell abstraction started at Day −90.

	Op. 1	Op. 2	Op. 3	Op. 4	Op. 5	Op. 6	Op. 7
Day	−64	−37	−20	149	257	511	588

sample tube volumes removed prior to sampling. Low water table conditions meant it was not always possible to sample all transect ports on all occasions.

In addition to the transect and monitoring well sampling data, other SABRE project data drawn upon included: (1) chlorinated ethene (TCE, cDCE, VC and ETH) concentrations measured at the abstraction well (used to constrain mass flow estimates through the cell); (2) *K* estimates from Hvorslev (Hvorslev, 1951) analysis of falling-head tests on T2a and T3a (used to provide initial estimates of *K* distribution at SW70 and SW75) (Cai et al., 2012); (3) conservative (bromide) tracer test breakthrough times at T2a (used to provide additional evidence of cell transport pathways away from the source zone). The conservative tracer test was undertaken from injection wells located 5 m upgradient of T2a (Dearden et al., 2010b). Monitoring at T2a was undertaken 14 times over the 25-day period of that test.

2.2. Numerical modelling approach

The aim of numerical modelling was twofold: to examine quantitatively inferences on SW70 and SW75 monitoring well sample origin via simulation of well capture zones based on the observed field data; and, to examine the groundwater quality samples which might have resulted had different sampling approaches been undertaken and hence to comment on sampling best practice. Modelled scenarios incorporate the field-observed heterogeneity in formation permeability and contaminant distributions. The numerical model assumes Darcy's Law flow within the aquifer and wellbore and does not consider the sensitivity to alternative wellbore flow representations (e.g., Poiseuille flow, viscous effects). These are examined for instance by Martin-Hayden et al. (2014) within a homogeneous aquifer setting to which the reader is referred.

Numerical modelling of the cell during the SABRE sampling operations was undertaken using MODPATH 5 (Pollock, 1994) and MT3DMS (Zheng and Wang, 1999) in conjunction with MODFLOW (Harbaugh et al., 2000) calculated specific discharges. The scope of modelling excluded direct simulation of the evolution of chemical concentrations in the cell between sampling operations. Rather, individual simulations of transient flow and transport during monitoring well sampling were undertaken separately for each SABRE sampling operation. TCE, cDCE and VC were all included in the numerical modelling. Particle tracking using MODPATH was used to assess advective well capture zones and compare simulated tracer test transport velocities to those observed in the conservative tracer test (Dearden et al., 2010b).

2.2.1. Model setup

The unconfined model domain (Fig. 2) is a simplified representation of the SABRE cell: the model domain is 29 m long, 4 m wide and 6 m deep and comprises 101 columns, 51 rows and 200 layers. The monitoring and abstraction wells are represented explicitly using a single column of very high *K* (10^6 m/d) cells. The high-K cells extend from the top of the model to the bottom of the screen interval of each well. The well casing is represented by MODFLOW's Wall boundary condition with a *K* value of 10^{-7} m/d and thickness of 0.01 m. The model grid is refined in the vicinity of the wells such that model well cross-sectional areas are equivalent to the real-world well dimensions. Grid refinement is reduced away from the wells up to a maximum row/column width of 0.13 m. Uniform layer spacing of 0.03 m is used between 1.5 and 6 m bgl. Above this, which for the majority of the model is above the water table, the layer heights incrementally increase up to a maximum of 0.4 m in the top layer.

The pump intake, located near the base of monitoring well screen interval in accordance with the field protocol, is explicitly represented using MODFLOW's well boundary condition. Simulated pumping rates were initially set to 1 l/min with sensitivity to increased (and decreased) pumping rate also investigated. Effluent discharge from the cell was simulated via a well boundary condition abstracting at a rate of 1.4 l/min placed in the middle of the screen interval location.

Transient sampling simulations were of 60-minute duration to allow examination up to and beyond the time to remove 3 well volumes (24 l) at 1 l/min. Changes in wider groundwater heads are assumed negligible

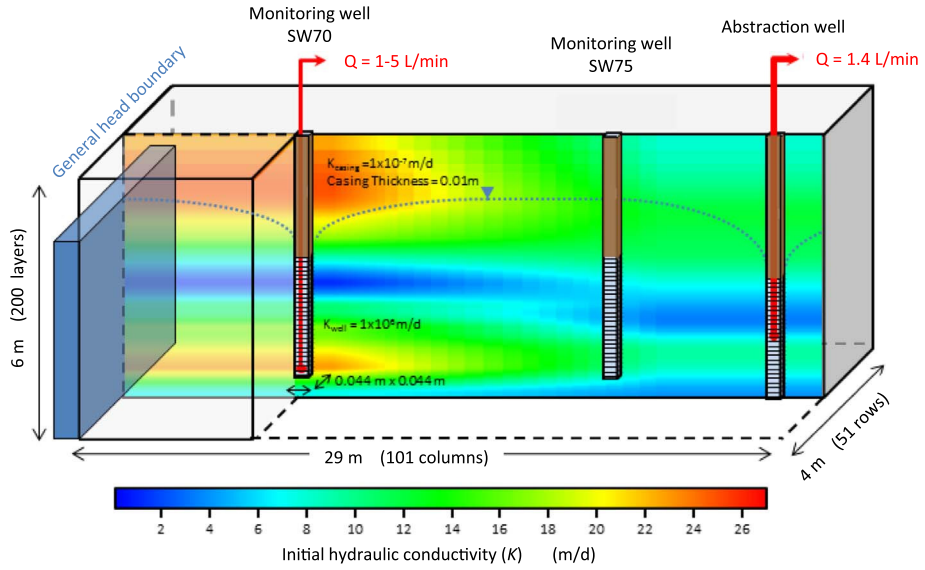

Fig. 2. Summary of model domain and parameters (not to scale).

over this short duration and hence the only model inflows are via a steady-state general head boundary (GHB) at the left-hand side of the domain. Recharge was assumed to be zero (cell was covered) and boundaries with the underlying aquitard and sheet pile walls assumed impermeable and hence assigned as no-flow boundaries in the model.

Observed heads in wells located immediately outside the cell remained roughly constant at *c.* 1.2 m bgl during SABRE cell operation. The right-hand GHB head is hence 1.2 m bgl with conductance configured (distance = 100 m, K = 0.5 m/d) such that initial heads at T2a and T3a matched those observed (*c.* 2 m bgl for T2a, *c.* 2.5 m bgl for T3a). The exception was during operations 5 and 7 when cell dewatering had resulted in decreased heads. For these simulations, the GHB was lowered to 2.2 m bgl such that the water table was *c.* 3 m bgl at T2a and *c.* 4 m bgl at T3a.

Extrapolation/interpolation of (falling-head test derived) hydraulic conductivity (K) and sampled T2a and T3a concentration data for each operation served to provide initial model K and chlorinated ethene concentration distributions that provided a representative source of dissolved-phase VOC concentrations surrounding and available to the pumped monitoring wells. The complexity of explicit representation of DNAPL dissolution was hence avoided (and considered not warranted for the study aim). Ordinary kriging was used to interpolate laterally across the cell at T2a and T3a and linear interpolation to assign values between the kriged K distributions at T2a and T3a. Upgradient of T2a and downgradient of T3a K and concentration distributions were extrapolated – these were assumed to be the same as T2a and T3a respectively (this is recognised to be a simplification, but not critical to the assessment of interactions local to the monitoring wells). For concentration kriging, non-detects were set to the detection limit and non-sampled ports were not included. Model porosity was set to the suggested cell average (0.25, Cai et al. (2012)). Specific yield and specific storage were chosen to be 0.1 and 0.0001 respectively. The heterogeneous K distribution in the model was assumed to account for large-scale (macro) dispersion. To simulate small-scale dispersive processes local to the monitoring wells, and to ensure model stability, model longitudinal dispersivity was set to 0.04 m (around 10% of local modelled capture zone radial distance over sampling timeframes simulated) and the transverse dispersivity to 10% of that value (0.004 m) (a standard assumption). Retardation due to sorption was reasonably ignored due to the low transport distances and timescales simulated (recognizing relatively low sorption is anticipated in high concentration DNAPL environments (Rivett and Allen-King, 2003)) alongside the modest difference in sorption potential between the chlorinated ethenes involved.

2.2.2. Model calibration and performance

Model performance was assessed by comparing the fit of simulated monitoring well sample concentrations with observed concentrations. Non-exhaustive manual calibration of T2a and T3a K distributions was used to explore improvement in model concentration fit statistics achievable through realistic, and constrained, adjustment of transect K values. Constraining T2a K adjustment involved comparison of tracer test peak arrival times to T2a with model simulated times to better define the velocity distribution through the transect. This resulted in greater weighting of faster flow paths traced by the test and hence their more prominent representation within the calibrated model. For T3a, adjustments in K-weighted estimates of total chlorinated ethenes mass flux through T3a were constrained by their expected equality with the overall cell abstraction well mass flux (equality of T3a water flux to the cell abstraction rate also being assumed). Spatial chemical concentrations interpolated from T2a/T3a were assumed fixed throughout the calibration process (albeit recognizing, similar to K, these may not fully represent actual conditions).

Summary residual statistics (root mean square error (RMSE) and residual bias) represented the overall model fit. These statistics were calculated using results from both monitoring wells, for all chemical components and operations:

$$RMSE = \sqrt{\frac{\sum_{o=1}^{7}(\sum_{c=1}^{3}(\sum_{w=1}^{2}(\hat{y}_{ocw} - y_{ocw})^2))}{42}} \quad (1)$$

$$Bias = \frac{\sum_{o=1}^{7}(\sum_{c=1}^{3}(\sum_{w=1}^{2}(\hat{y}_{ocw} - y_{ocw})))}{42} \quad (2)$$

where o is the operation (1–7), c is the chlorinated ethene component (TCE, cDCE or VC), w is the monitoring well (SW70 or SW75), $\hat{y}_{ocw}$ is the modelled sample value for a particular operation, chemical and monitoring well and y_{ocw} the observed sample value.

The field protocol involved SW70 and SW75 being purged for a minimum of 3 well volumes (typically 4 screen volumes) with inline water quality parameters allowed to stabilize before sampling with hence some variation of purge times possible. Model simulations simply assumed a purging time, greater than the time to remove 3 well volumes (*c.* 24 min being a typical timeframe). For each set of model parameters, calibration results were reported at 5 min intervals assuming purging times between 25 and 60 min. Plotted simulated

Table 2
Predictive modelling scenarios simulated.

	Scenario 1	Scenario 2	Scenario 3	Scenario 4
Pumping rate (l/min)	2.5	1	0.3	0.3
Pump intake location (within screen interval)	Bottom	Bottom	Bottom	Top

estimates used the purging time result at which overall residual summary statistics were minimised.

2.2.3. Predictive modelling

Predictive modelling using a non-exhaustive range of scenarios (Table 2) was undertaken with the aim to investigate the effect pumping rate, pumping time and pump intake position might have had on monitoring well sample concentrations in the SABRE cell. Pumping rates were selected to span a range from low-flow (0.3 l/min) to higher (1 and 2.5 l/min), but not untypical, rates used to sample 3-m screen monitoring wells. Predictive modelling was undertaken using the final calibrated *K* distribution resulting from the observed monitoring well data fits.

3. Results and discussion

3.1. Observed MLS transect and monitoring well data

Orders of magnitude variation in concentration was observed across the MLS transects T2a (Fig. 3) and T3a (Fig. 4), both spatially and with time. Proximity to the heterogeneous DNAPL source and weakness of transverse dispersion are probable key factors leading to this high level of variability. Total (not shown) and individual chlorinated ethenes could locally and sometimes extensively approach literature TCE molar solubility values (*c.* 8400 to 10,700 μM) and accords with close proximity of MLS points to the DNAPL source zone. T3a generally exhibited greater concentrations at depth (> 4 m bgl) with T2a presenting a more complex distribution with low concentrations of TCE above 4 m bgl contrasting with elevated cDCE values. The reverse distribution is observed below 4 m bgl.

Chlorinated ethene concentrations remained relatively stable during the baseline period (Operations 1–3). Whilst daughter products were observed in both transects, their relative occurrence was variable across the cell. A comparative absence of TCE above 4 m bgl in T2A was observed (Fig. 3) with increased cDCE. By contrast, below 4 m bgl, relatively high TCE concentrations remained with daughter products making up a much smaller contribution to total chlorinated ethene mass. Variation laterally across transects was marked in some cases and absent in others where concentration appeared more layered.

Monitoring well concentrations were relatively stable over the baseline period (Fig. 3 and 4, Op1 – Op3). SW 70 concentrations of TCE at 1765–1826 μM were elevated compared to cDCE at 649–835 μM and VC at 176–320 μM. The relative increase in daughter products in the upper half of T2A during the baseline conditions was not reflected in SW70 samples (Fig. 3). SW75 baseline samples were similarly reflective of the higher chlorinated ethene concentrations observed in the lower half of T3a rather than the low concentrations observed above 4 m bgl (Fig. 4). Total molar chlorinated ethene concentrations at both SW70 and SW75 during the baseline (not shown) were > 10% of the TCE molar solubility and hence provided some endorsement of the so-called > 1–10% solubility rule of thumb (Pankow and Cherry, 1996; US EPA, 1992) often used by practitioners to be indicative of possible presence of DNAPL upgradient.

During bioremediation, enrichment in dechlorination daughter products and depletion of TCE were observed in both monitoring wells and MLS transects (Figs. 3 and 4, Op4 – Op7). Total chlorinated ethene molar concentrations observed, even in monitoring well samples, approached or exceeded TCE molar solubility. This could potentially reflect enhanced dissolution effects at the site (Rivett et al., 2014).

K distributions measured at T2a and T3a were heterogeneous (Fig. 3 and Fig. 4). Hydraulic conductivity was generally greater within transect T2a (< 1 to 28 m/d) than within transect T3a (< 0.1 to 14 m/d). Values were also generally larger in the upper alluvium (above 2 m bgl). Marked variation in *K* was apparent in the poorly-sorted river terrace gravels at depth with an area of higher *K* observed in both transects at 5 m bgl. This high K zone appeared restricted to the right-hand-side of the cell at T2a but extends the full width of the cell at T3a.

3.2. Provenance of monitoring well samples

Pumped monitoring well samples as a first approximation may be expected to yield a FWA of adjacent formation concentrations. Occasional observations were made of monitoring well concentrations approaching minimum or maximum concentrations recorded within adjacent transects (Figs. 3 and 4). It is usefully inferred from such occurrences that sample provenance must be strongly biased towards similarly high, or low, concentration zones found in the adjacent formation with little contribution to the sample concentration from other parts of the transect. Hence, SW70 sample provenance was strongly biased towards the highly conductive zone towards the lower right-hand side of the cell. Although less clear for SW75, the data generally support sample provenance was from the more permeable formation at depth, but less strongly biased towards the right-hand side of the cell than encountered for SW70.

The provenance of monitoring well samples is further evaluated in Fig. 5 where observed monitoring well concentrations are plotted against calculated well concentrations based on MLS transect *K*-weighted concentrations. *K*-weighted concentration estimates from the MLS ports directly down gradient spanning the vertical screen interval (solid circles in Fig. 5b and g), that potentially represented the most appropriate FWA concentration estimate available, provided only moderate prediction of observed SW70 and SW75 sample concentrations (Fig. 5c and h). *K*-weighted concentrations using selectively sampled concentrations drawn from the high *K* zones in both T2a and T3a (dashed circles in Fig. 5b and g), provided much improved predictions of observed monitoring well concentrations for chlorinated ethenes (Fig. 5d and i) as well as for chloride and sulfate (Fig. 5e and j) for which a particularly good fit was observed with very low RMSE and bias values calculated. Our preliminary conclusion is that well inflows were more complex than can be judged from simplistic consideration of the *K* distribution corresponding to projected location of the well on the upgradient transect. The monitoring well sample is likely to have contributions from across the screen interval; however, *K* contrasts are such that these contributions appear to be dominated by inflows from the highest *K* zone(s) at depth. Furthermore, 2 or 3-dimensional, rather than simple 1-dimensional, information is required to assess the sampling interaction of the monitoring well with its surrounding formation.

3.3. Monitoring well sample bias towards preferential transport pathways

Temporal variance across sampling operations was not uniform in space (Fig. 5b and g). Particularly for T2a, and to a lesser extent T3a, areas of the MLS transect associated with smaller changes in concentration with time generally coincided with areas of lower *K* (Fig. 5a and f) and, conversely, greater temporal changes were generally associated with zones of higher K. The more permeable horizons act as preferential pathways for transport away from the source zone, and thus reflect enhanced concentration variation resulting from changes to DNAPL dissolution caused by bioremediation. Because monitoring well results are weighted to reflect conditions within preferential transport pathways, SW70 and SW75 likewise sample concentrations exhibiting a relatively high temporal variance (Fig. 5, note coloration of well screen depicts temporal variance of well samples). Such monitoring well

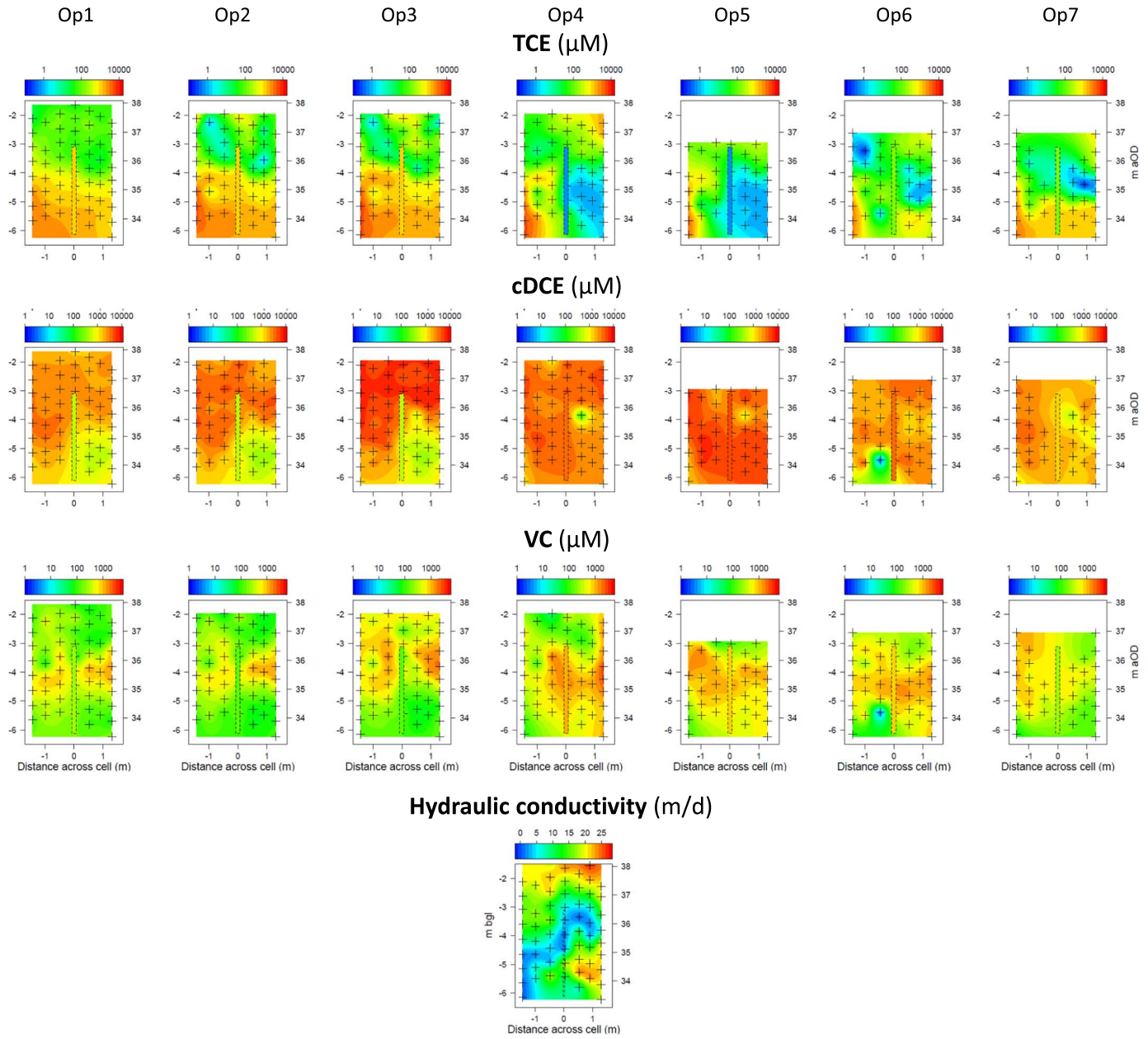

Fig. 3. Kriged MLS transect T2a TCE, cDCE and VC concentrations compared with SW70 monitoring well sample concentration (concentration shown as uniform over dashed line screen interval with radius increased by a factor of 3 to enhance visibility) with kriged transect *K* shown for comparison. Concentration data are shown for the baseline period sampling operations (Op. 1 to Op. 3) and for the bioremediation phase (Op. 4 to Op. 7). Groundwater flow is normal to the page (transect) towards the reader.

observations further underscore the importance of the high-K zones contributing to monitoring well sample provenance and suggest that the monitoring wells usefully reflect concentrations occurring in pathways that are important to VOC transport through the test cell.

The significance of spatial continuity of the high-*K* zone at *c*. 5 m bgl towards the lower right side of T2a is further highlighted by the bromide tracer test (contoured in Fig. 6; breakthrough Supplementary material Video V1). Fastest breakthrough at T2a (< 0.25 d, Fig. 6) and peak tracer concentrations were each observed in this high-K zone. Analysis of a plume longitudinal snapshot sample along the cell length at 6 days (not shown) confirmed tracer had migrated 25 m down the cell and confirmed maximum and mean cell velocities of 3–4 m/d and 2.1 m/d respectively (Rivett et al., 2014). Such velocities resulted in estimates of minimum and mean travel times between SW70 and the abstraction well of 4.25–5 d and 8.1 d, respectively. Travel times from SW75 to the abstraction well are approximately one quarter of those from SW70 to the abstraction well. These times are much shorter than those predicted from the nominal cell pore volume calculation earlier and again point to the continuity and significance of localized preferential flow paths along the cell length.

The concentrations (as total moles of parent and daughter products) measured at abstraction wells that captured the cell effluent, and hence expected to be indicative of a *K*-weighted average concentration moving through the bulk cell, reasonably compared to those measured at SW70 and SW75 during both the baseline and bioremediation phases (Fig. 7a). This is noteworthy given the orders of magnitude variation in concentration observed within the T2a and T3a transect points, and provides a further line of evidence that the monitoring well samples may be reasonably representative of the overall bulk concentration dissolving from the DNAPL source zone and transported through the cell.

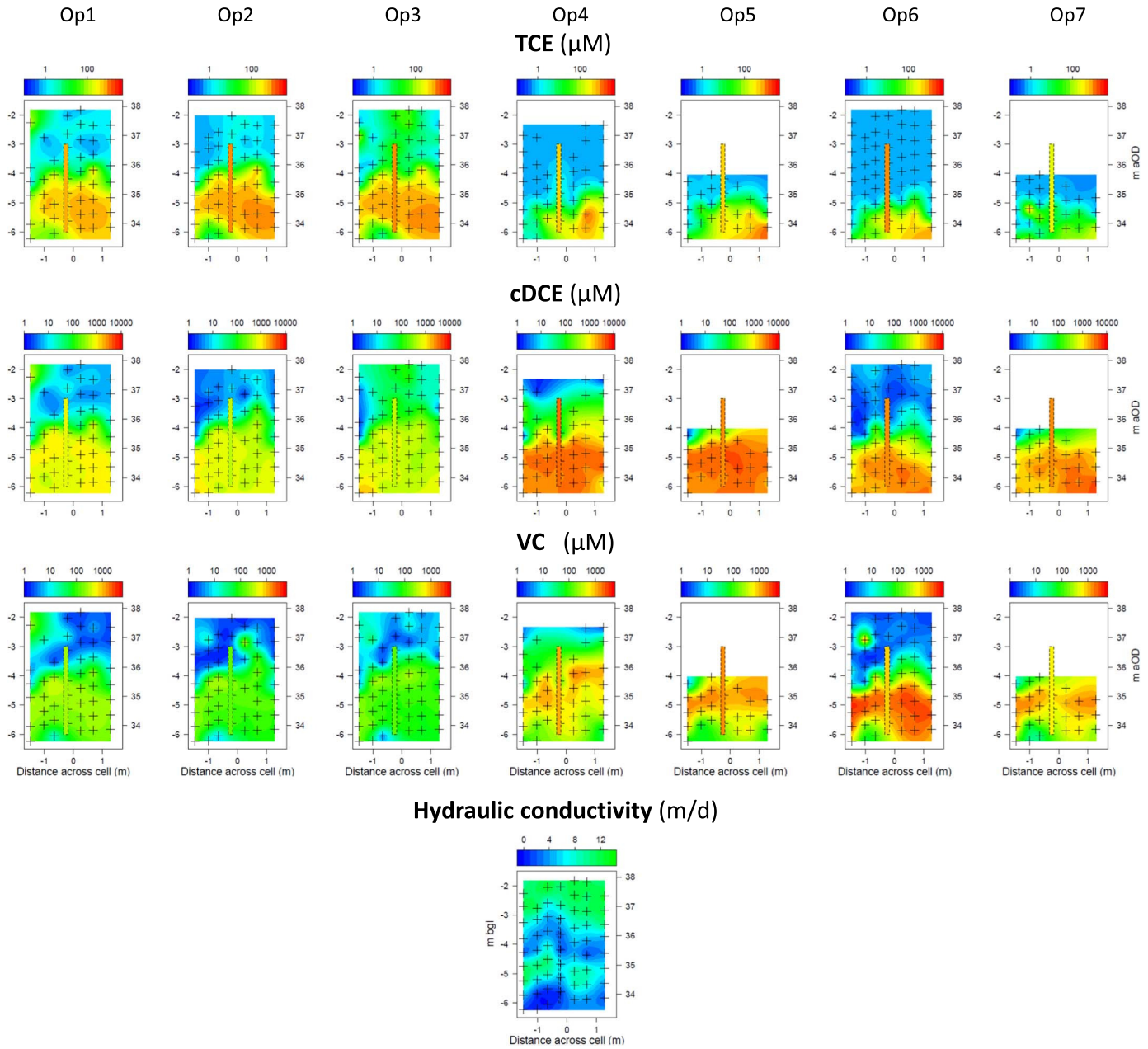

Fig. 4. Kriged MLS transect T3a TCE, cDCE and VC concentrations compared with SW75 monitoring well sample concentration (concentration shown as uniform over dashed line screen interval with radius increased by a factor of 3 to enhance visibility) with kriged transect *K* shown for comparison. Concentration data are shown for the baseline period sampling operations (Op. 1 to Op. 3) and for the bioremediation phase (Op. 4 to Op. 7). Groundwater flow is normal to the page (transect) towards the reader.

3.4. Numerical modelling results

Numerical modelling of individual monitoring well capture zones provided additional insights into sample provenance. Simulated sample concentrations for purge times of 24 to 60 min were compared with observed data (not shown). The best match to monitoring well sample concentrations was obtained after 30 min of simulated pumping and is shown in Fig. 8c, g for cell simulations based on the observed (uncalibrated) *K* distribution interpolated/extrapolated from T2a and T3a data. For SW70, the matches with observed TCE and VC were generally good, however, cDCE concentrations were overestimated. For SW75, TCE concentrations were underestimated particularly in operations 4 to 7. Model predictions using the observed *K* distribution were similar to those obtained by averaging directly upgradient port concentrations (Fig. 5c and h); insufficient weighting (importance) appeared to be allocated to well inflows from the high-*K* zone at 5 m bgl to generate the concentrations observed at the monitoring wells.

Use of calibration model *K* distributions (Section 2.2.2) allowed improved monitoring well concentration matches to be obtained (Fig. 8). Transect T2a *K* calibration (used for well SW70 predictions) was constrained by use of the tracer test velocity estimates (Fig. 6); and T3a *K* calibration (used for well SW75 simulations), by improved prediction of the overall cell abstraction mass flux from T3a mass flux data (Fig. 7b). The calibrated model *K* distributions achieved are shown (Fig. 8b, f) to retain the style, for the most part of the field-observed K distributions (Fig. 8a, e; (see later discussion of T3a departure). Improved simulation of observed concentrations using the calibrated *K* model (Fig. 8c compared to Fig. 8d; Fig. 8g compared to Fig. 8h) was largely ascribed to the relative accentuation of flows to monitoring wells from the inferred preferential flow zones located to the lower right-side of each transect in the calibrated model compared to flow regimes simulated with the observed *K* distribution. The accentuation

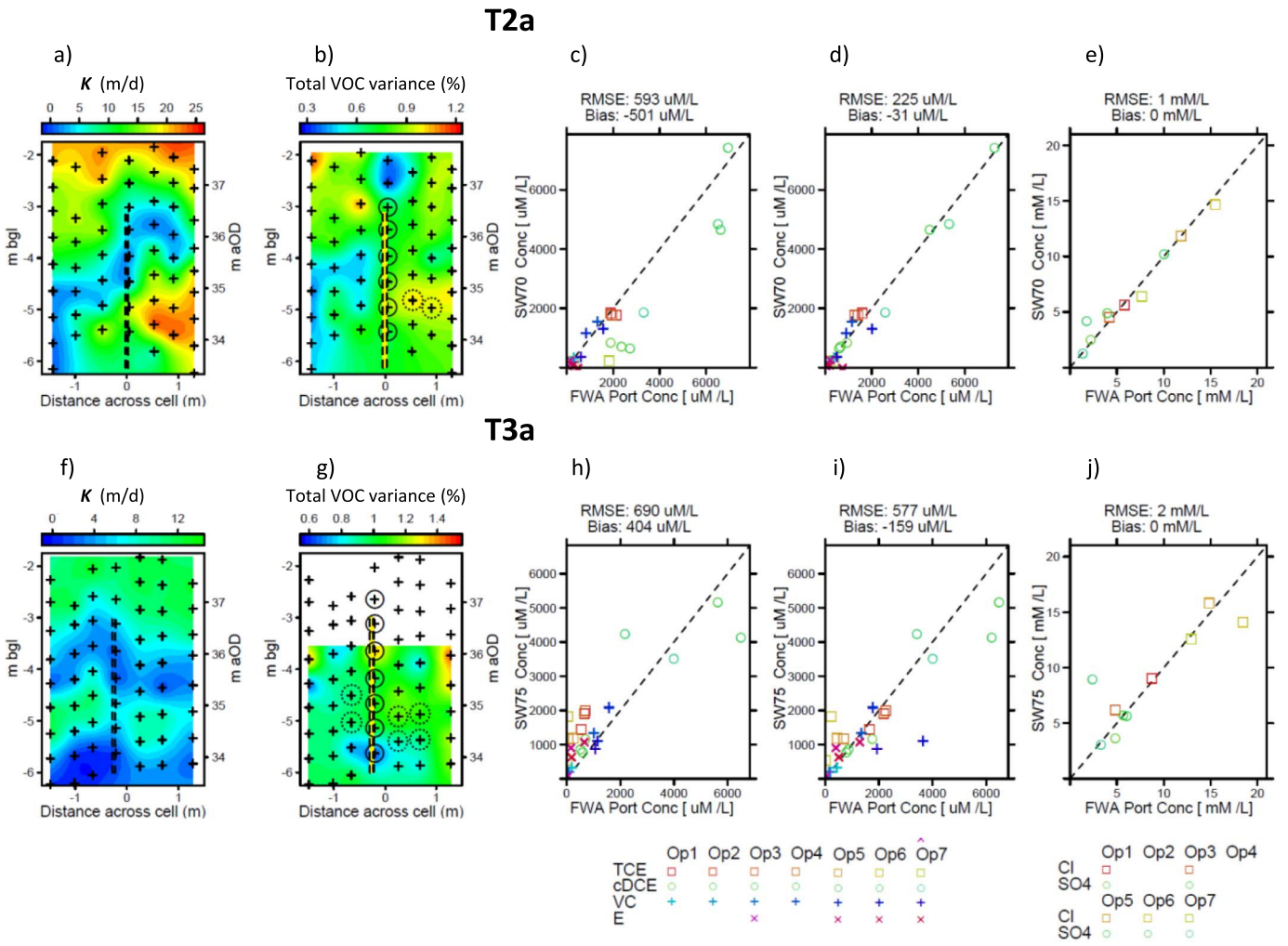

Fig. 5. Provenance of monitoring well samples: T2a and T3a *K* distribution (a, f); temporal variance in total chlorinated ethene concentrations (b, g); predicted flow-weighted average (FWA) transect port chlorinated ethene concentration compared to observed monitoring well concentration data (c, d, h, i). For c) and h), ports used lie directly upgradient of the monitoring well screen interval (solid black circles in b) and g)); for d) and i) ports used are from the high *K* zone at 5 m bgl (dashed black circles in b) and g)). e) and j) show chloride and sulfate results for the high *K* (dashed circle) ports.

of preferential flows invoked within this part of the T2a transect is corroborated by the rapid breakthrough of much of the tracer in this zone at 1–2 d (Fig. 6). This time compares to the calibrated model estimate of 2.7 d, but is significantly below the observed *K* distribution model estimate of 7.9 d.

The difference in monitoring well simulated capture zones between observed and calibrated model *K* distributions assumed is shown in Fig. 9. The difference is more significant in SW70 (compare Fig. 9a and b) and illustrates the *K* distribution caused the majority of the sample to be drawn from the lower half of the screen interval, even after 60 min. After 15 min of pumping (removal of 2.5 screen volumes) from SW70 and SW75, the well capture zone had still not spread to encompass the entire screen interval. The elapsed time (as screen volumes purged) until a screen-integrated sample is achieved depends on the relative volumes of water entering different parts of the screen and translocation to the pump intake: this volume is a function of screen inflows (and therefore the *K* distribution).

Sensitivity testing confirmed that the simulated monitoring well concentration was relatively insensitive to the model *K*-distribution in regions not immediately adjacent to the screened interval (both laterally and above the screen interval). Rather, it was the local relative contrast in *K* immediately adjacent to the screen interval that assumed most importance in determining the contribution to sample concentration from different parts of the screen interval. The *K* value of the low-*K* zones adjacent to the upper screen interval in both SW70 and SW75 (Fig. 8a, e) were similar. However, the contribution to the pumped sample from the low *K* zone adjacent to SW70 is much smaller (reduced sample distances travelled) than that from the low *K* zone adjacent to SW75 (Fig. 9). This is ascribed to the greater (a factor of *c.* > 2) permeability contrast adjacent to the screen at depth in SW70 compared to SW75. In determining well inflows, it is hence the relative difference in permeabilities occurring across a screen length that is important and not the absolute values. The connectivity of the more permeable zones adjacent to the well screen with the distribution and orientation of permeable horizons, more remote from the well, but immediately surrounding and supplying inflow to these zones, is assumed to influence the wider sample provenance.

Observed abstraction well total chlorinated ethenes mass flux rates for all but two of the sampling operations (Op 5 and Op 7) were significantly underestimated using the observed T3a *K* distribution to provide a Darcy flux – concentration based estimate of chlorinated ethenes mass flux through this transect (Fig. 7b). This was despite a relatively high sampling density at T3a (3.75 points/m^2) (Cai et al., 2012). Observed T3a *K* distributions excessively weight abstraction well contributions from the top half of the cell. Improved matches for Operations 5 and 7 were attributed to low water levels and corresponding absence of flow and mass from higher elevations. A good match to abstraction well mass flux estimates across all operations

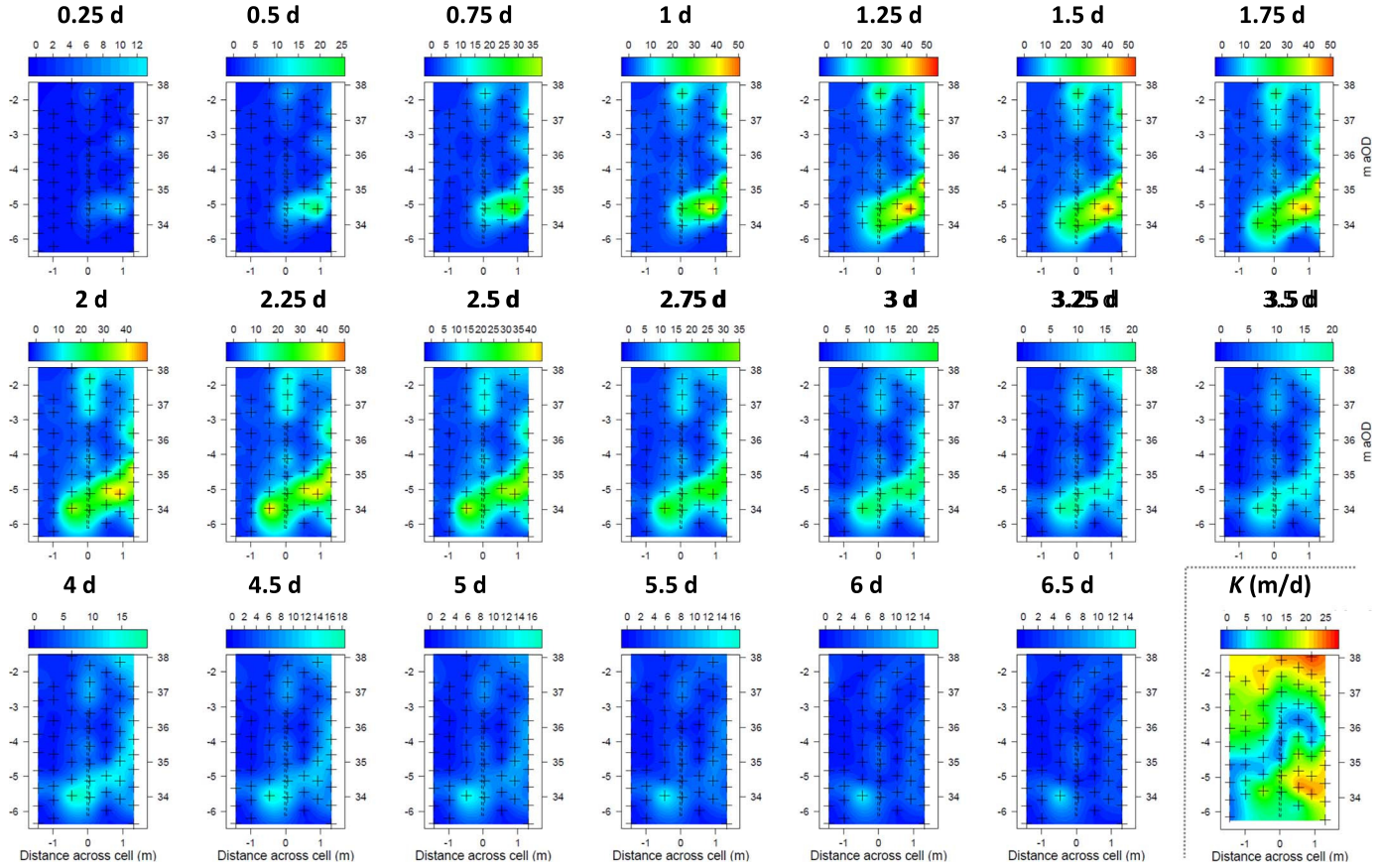

Fig. 6. Bromide (mg/L) tracer test breakthrough observed at transect T2a up to 6.5 d with inset showing K distribution at T2a. Tracer was introduced 5 m up-gradient of T2a via recirculation in the three tracer injection wells (Fig. 1). Breakthrough monitoring continued until 45 d, but with no further significant breakthrough.

(Fig. 7b) was achieved only after model calibration which almost entirely excluded flows to the abstraction well from the upper half of the cell at T3a by assuming substantially reduced permeability at upper cell elevations of T3a (compare Fig. 8f to Fig. 8e).

The probable reality is that continuity of the low-K layer in T3a at 3 to 4 m bgl (Fig. 8e) limited shallow groundwater flows to the cell abstraction well screen. This interpretation is endorsed by: distinct chlorinated ethene concentrations above and below 4 m bgl in T3a; and, cross cell hydraulic heads recorded in T3a where heads were consistently higher above 3.5 m bgl (Supplementary material, Fig. SM1). It is conceptualized that some leakage of shallow groundwater may occur across the low-*K* layer with associated convergence of flows and contamination into the deeper, screened, aquifer. Dominant flows are, however, through the permeable cell horizons at depth. Such conceptual understanding is consistent with interpretations hitherto made of flows sampled by the monitoring wells (and core lithological data (not shown)).

3.4.1. *Predictive modelling of alternative sampling strategies*

Simulation of long time (> 3 screen volumes (SV) purged) sampling suggest that monitoring well sample concentration in SW70 and SW75 was insensitive to the pumping rate and pump intake positions used (Fig. 10). This result is expected given steady-state screen inflow rates dependent on the variation in *K* local to the screen interval. As groundwater from contributing horizons reaches the pump intake a quasi-steady state mixing is achieved, regardless of pumping rate and pump intake location in SW70 and SW75. This is further explained in Fig. 11a and Fig. 11b which show similar well inflow profile variability with depth for the various pump rate and positions simulated. The exception was if drawdown was sufficient to drop water levels below the screen interval. During Operations 5 and 7, cell water levels were within the screen interval at SW75. For these two operations, the long-time screen inflows depended on the pumping-induced drawdown in the well and hence the pumping rate (Fig. 11c). Interestingly, while screen inflows varied with pumping rate during Operations 5 and 7 in SW75, simulated SW75 monitoring well concentrations varied little (Fig. 10). This lack of simulated sample concentration variation with pumping rate is attributed to: the small contribution to total screen inflow from the top half of the screen (due to bias towards the high-K zone at 5 m bgl); convergence of flow from higher up in the formation towards the well (as evidenced by the small peaks in the inflow profiles at the water level in Fig. 11c) meaning groundwater from higher in the aquifer still makes a contribution to sample concentration.

Early time (< 3 SV) simulated sample concentration was independent of pumping rate but did depend on the pump intake position (Fig. 10). If a large concentration contrast existed across the screen interval (e.g. Op 1 TCE Fig. 3 and Fig. 4) differences in early time simulated sample concentrations as a function of pump intake position were large. Where little or no concentration contrast existed with depth (e.g. T3a VC concentrations during Op1–3; Fig. 4) variation in sample concentration with pump intake location was small or negligible (Fig. 10).

The variation in simulated sample concentration during very early times was significant, particularly over < 1 SV purged (by 1–2 SV, variation was more limited). This was also a function of the variation in chlorinated ethene concentration with depth adjacent the screen interval. Greatest sample variation with time occurred when variation in chlorinated ethene concentration across the screen interval was high (e.g. during Ops 1–3 for SW70, Fig. 3; Fig. 10). Pump intake location can also be important in early-time sample variation. The greatest change in simulated sample concentration with time occurred when starting concentrations were very different from the *K*-weighted, long-

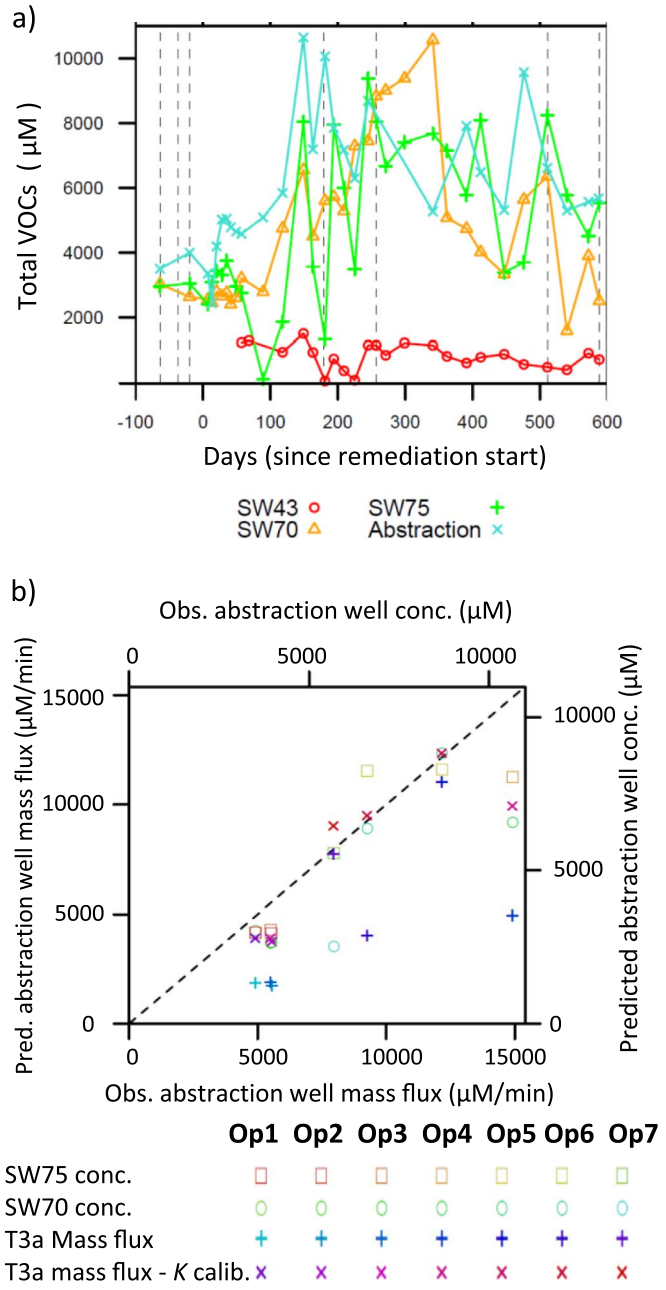

Fig. 7. a) Temporal total chlorinated ethenes in SW70, SW75, cell abstraction well and SW43 (upgradient of cell entrance) with Op1 – Op7 events shown by dashed lines; b) use of SW70, SW75 and T3a as predictors of observed total chlorinated ethene concentration and mass flux at the cell abstraction well. T3a fluxes are calculated using kriged *K* (slug test) and concentration distributions that assume perpendicular flow through T3a proportional to *K* with total flow equivalent to the cell abstraction rate (1.4 l/min); T3a mass flux (*K* calibrated) estimates are calculated using the numerical model calibrated T3a *K* distribution.

time average (e.g. SW70 cDCE, Ops 1–3, Fig. 3; Fig. 10). It can hence be reasonably inferred monitoring well sample concentrations obtained during low-flow purging (and indicator chemical parameter stabilization) that involves removal of low volumes (around 1 SV or less), will be very sensitive to pump intake position, especially where marked variability of concentrations occurs with depth; a default expectation, and hence issue, for DNAPL source-zone areas. Concentration sensitivity over < 1 SV purged (but extending up to around 2 SV or more) is similarly predicted by Martin-Hayden et al. (2014) even under homogeneous aquifer conditions alongside secondary sensitivity to the wellbore flow representation modelled.

In our model, the initial well contaminant distribution reflected that found in the immediately upgradient multilevel. Assuming different initial conditions within the wellbore would clearly influence early-time (< 1SV) sampling predictions, however, the analytical solution of Martin-Hayden (2000) suggests that the relationship between early time sampling variability and near-screen vertical stratification in contamination remains, even if the wellbore is assumed to be fully mixed. This raises the possibility of using early time variations in sample concentration as an indicator of contaminant variability. This, though, is likely impractical due to the inadequate timeframes to complete the collection of multiple early-time samples required.

Prior studies suggest purging of 3 SV is likely sufficient to obtain a quasi-steady state sample from a monitoring well; for example, the modelling of Martin-Hayden et al. (2014) to account for partial mixing and transport times to the pump, and the modelling of McMillan et al. (2014) to account for the delayed arrival of casing water at the pump. Our predictive model simulations support these prior conclusions. After removal of 2–3 SV, early time variations in sample concentration (due to the influence of pump intake location or vertical contaminant stratification) have largely been resolved with relative stability achieved as formation water is drawn from across the screen interval (Fig. 9). Furthermore though, we also show that in such heterogeneous DNAPL source zone environments, a lower level of variability may persist beyond 2–3 SV (Fig. 10). This long-term variation was attributed to the arrival of more distant formation water of different concentrations to the pump intake location. Dispersion meant changes with time became less pronounced, but it is likely that a truly stable sample concentration may not be attained.

4. Conclusions

Establishing the utility of short-screen monitoring wells within heterogeneous DNAPL source zones is important due to the widespread continued use of wells. This is despite the availability of higher resolution technologies. Where heterogeneity and vertical head gradients are low, monitoring well samples are weighted by vertical variations in hydraulic conductivity local to the screen. At long sampling times corresponding to > 3 screen volumes (SV) purged, a quasi-steady state flow condition is approached where the FWA concentration sample becomes independent of pump rate and intake position. At early times, however, purged sample variability depends upon chemical stratification adjacent to the screen and the difference between initial well and long-time FWA concentrations. In chemically heterogeneous environments, true sample chemical stability may never be reached. Where geological permeability varies over orders of magnitude, mass flux from the high permeability zones will tend to dominate and sampled concentrations reflect contamination from these transmissive zones. This was the case at the SABRE site where monitoring-well concentrations sampled the dominant aquifer contaminant flux and provided a representative indicator of dissolution and transport from the DNAPL source.

It is hence concluded that careful well design and the development of bespoke monitoring protocols are needed to validate data from short-screen wells used to monitor source zone areas. Individual well protocols are particularly merited here due to the greater contamination heterogeneity expected relative to areas more distant from the source area. Although expensive to develop, such protocols may ultimately prove cost-effective as risks of prolonged employment of inappropriate protocols are lowered. Samples will exhibit sensitivity to the adopted protocol and the degree of purging undertaken as a consequence of the varying degree of heterogeneity (permeability and contaminant) adjacent to a well screen, pump-intake position and water level. Protocols involving sampling after purging of low screen volumes (particularly up to 1 SV, and potentially 2 SV) may be vulnerable to poor repeatability as a consequence of marked sample concentration variability over these purged volumes. This is particularly true where formation

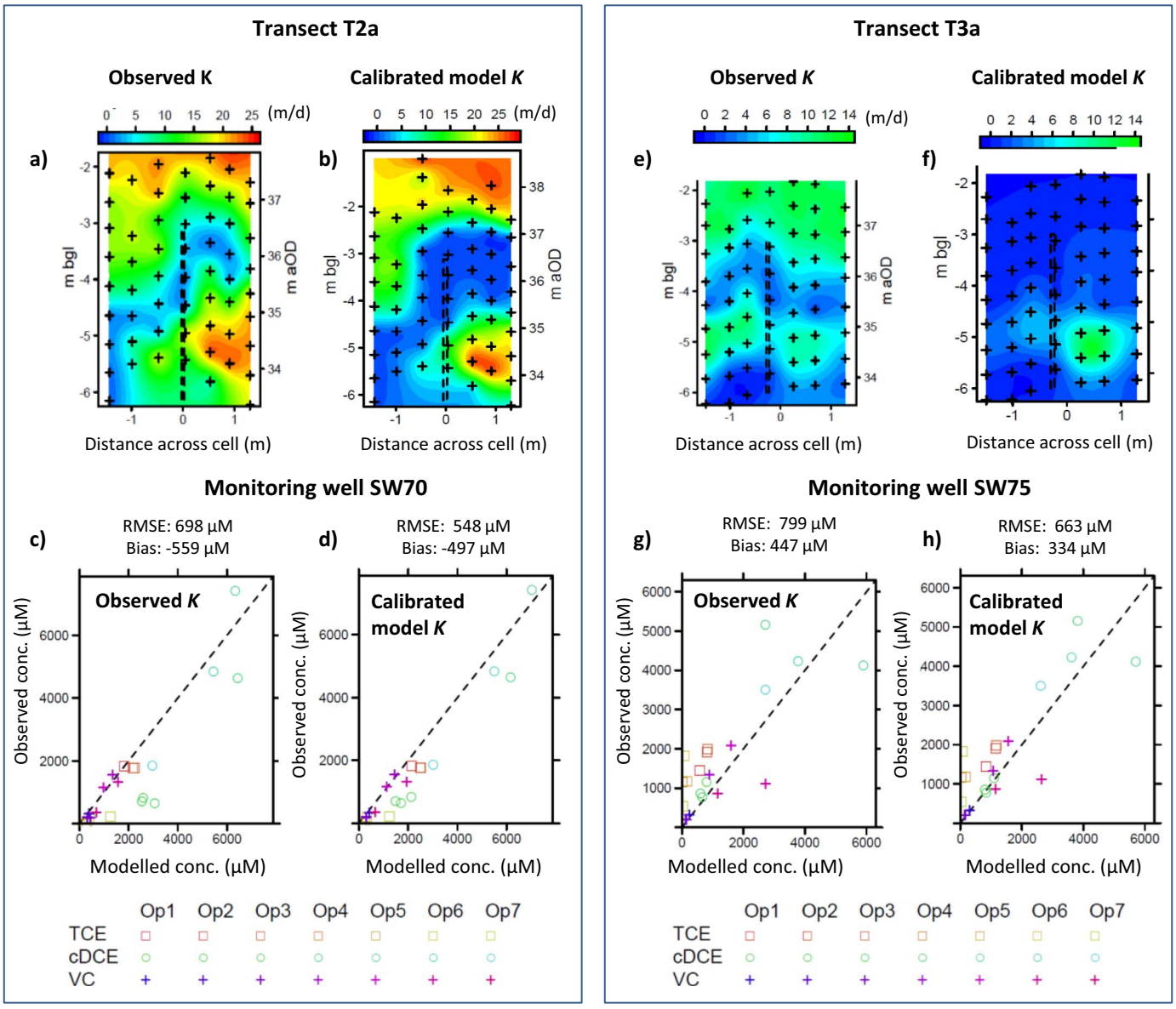

Fig. 8. Simulated versus observed monitoring well sample concentrations comparing results using shown observed transect *K* and calibrated model *K* distributions. Samples are taken after 30 min pumping at 1 l/min for which RMSE and bias for best fit transect ports (Fig. 5b, g) were: 225 uM and 2 uM respectively for SW70; 644 uM and −212 uM for SW75) in the final calibrated model *K* distributions used (Fig. 8b, g).

contamination varies markedly with depth; indeed, a default expectation at DNAPL sites. It is inferred here that zero/minimal-purge sample concentrations may be sensitive to sampler positioning in the well screen and the presence of any distinct stratification of contamination. Where high temporal concentration sensitivity is apparent over a < 1SV purge (and probable at DNAPL sites), this may not unreasonably translate to an expectation of high sensitivity of zero/minimal-purge sample concentrations to deployment depths (and vice versa). There would be an onus to evaluate the degree of in-well mixing and contaminant redistribution versus contaminant stratification (Britt et al., 2014) to justify adoption of a depth-specific zero/minimal-purge type sample protocol.

Low-flow sampling protocols typically advocate sampling after stabilization of well-head parameters as an indicator of representative formation water fluxes (US EPA, 2017), but do not specify a minimum number of screen (or well) volumes to be purged. In view of the lack of sensitivity of typical well-head parameters to dissolved-phase DNAPL-contaminant presence, we recommend low-flow sampling protocols should also routinely record a minimum number of screen volumes to be purged to quantify the degree of purging undertaken. This work suggests 1 SV at minimum, 2 SV to allow good sample confidence and 3 SV to allow high sample confidence (recognizing decreasing time efficiency and cost effectiveness). The objective being to ensure sampled water is in quasi-steady state interaction with the formation. Such volumes are consistent with the recommendations of Martin-Hayden et al. (2014) who illustrate a 'partial purge' condition may persist over *c*. 3 SV. In passing, we concur with the recommendation of Martin-Hayden et al. and Robin and Gillham (1987) that where the pump intake is positioned within the well screen and there is insignificant drawdown, screen volumes should be used as the unit-of-measure for quantification of purging as they are technically more defensible than well volumes and constant with time.

As introduced earlier, there is debate between potentially onerous low-flow purging of multiple screen volumes and the comparative ease of zero/minimal-purge sampling, but also a recognised need to aim for consistency in monitoring-well sampling approaches. Protocols should aim to capture the key concentration features and avoid undue or unknown sensitivity of concentrations to sample depth or purge time. This

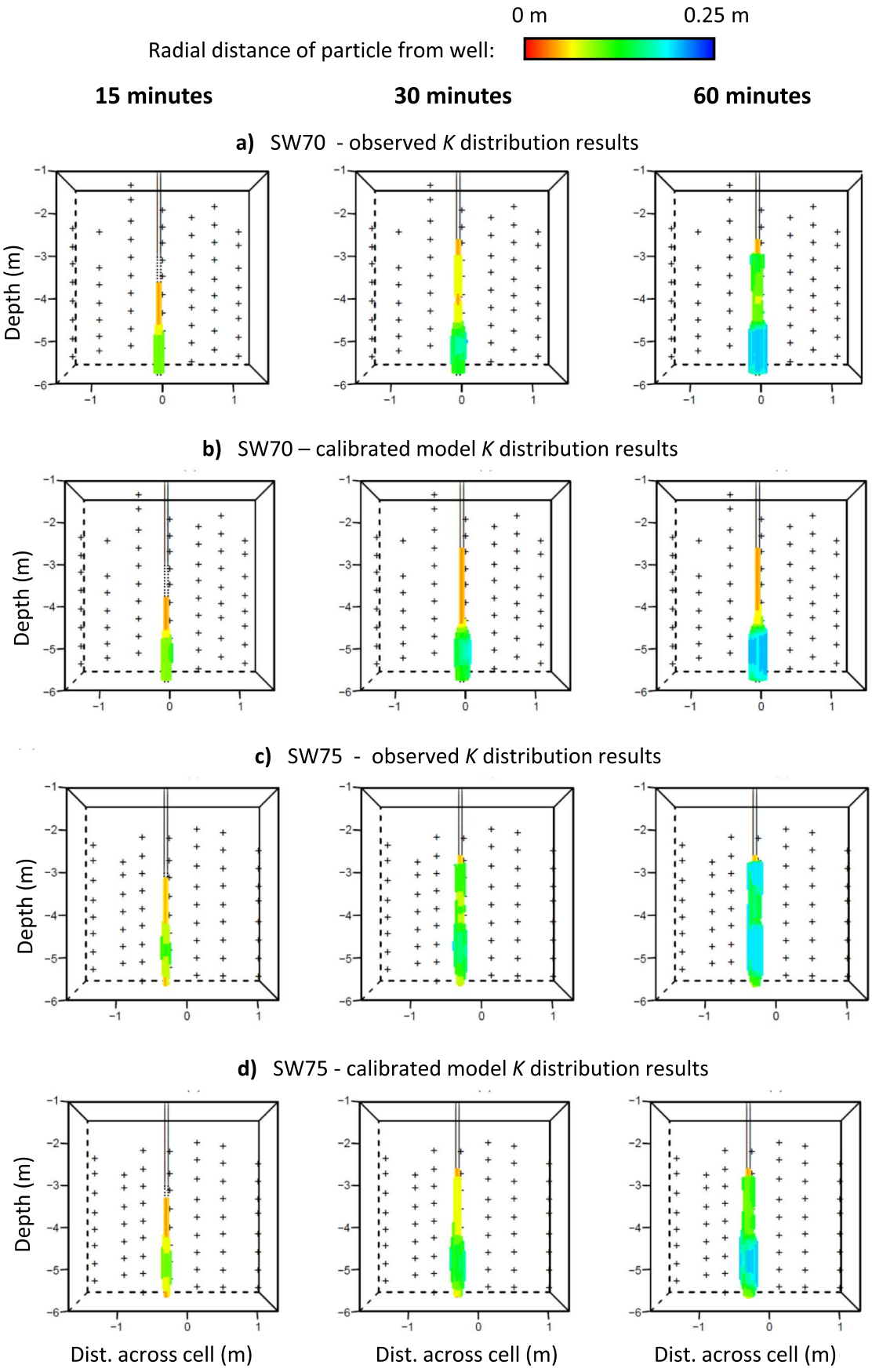

Fig. 9. Monitoring well SW70 and SW75 simulated pumped capture zones for initial model *K* and scaled *K* distributions after 15, 30 and 60 min of pumping (2.5, 5 and 10 screen volumes) at 1 l/min.

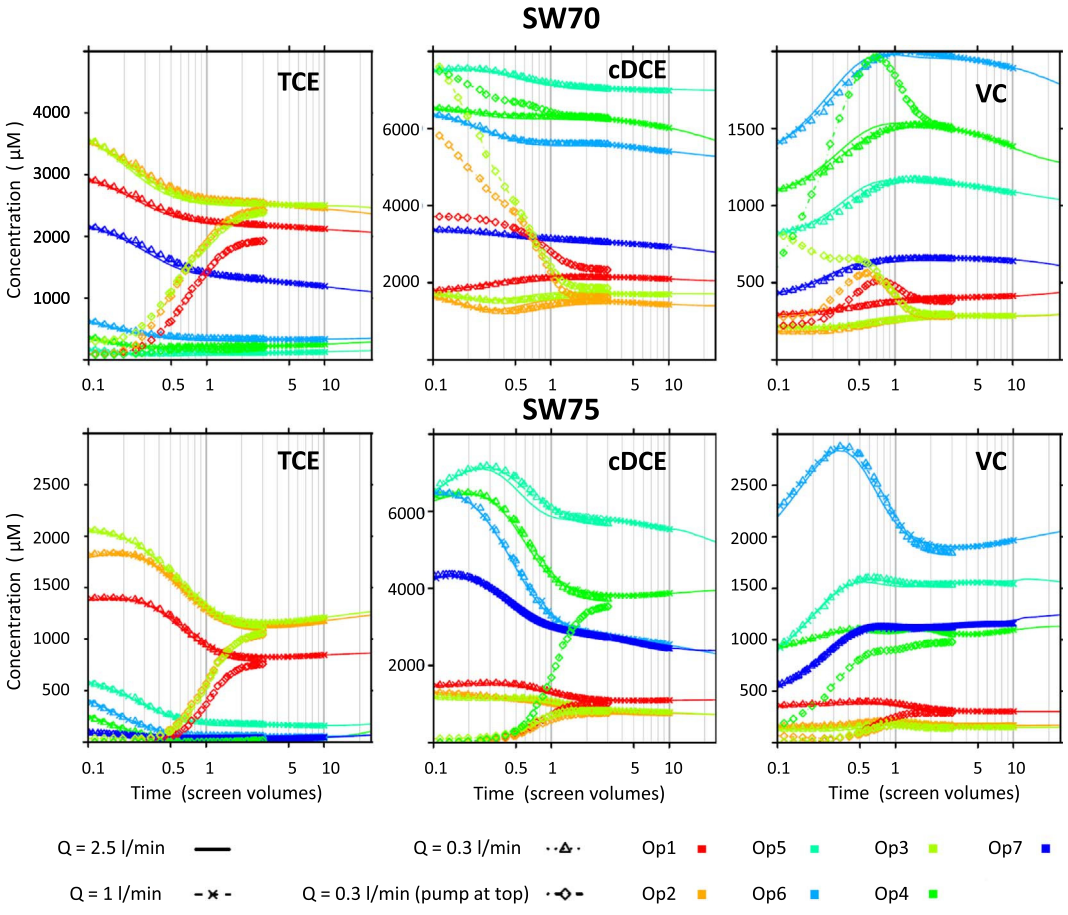

Fig. 10. Simulated SW70 and SW75 monitoring well sample concentrations as a function of pumping rate, pumping time and pump intake position (for calibrated model *K* distribution). Data point/line colour indicates the sampling operation with symbol style corresponding to pump rates shown.

is challenging in DNAPL source zone areas; however, our generalised recommendations for monitoring well-based protocols that are pragmatic for such environments include:

- Protocols should be developed bespoke to individual wells but aim to have commonality among wells where possible.
- Pumped samples using low flow rates should ideally only be taken after purging at least 1 SV to overcome much of the expected initial sample concentration variability. However, the potential for concentration temporal variability should be initially, and occasionally, examined by sampling over 2–3 SV purged or more. Purged volumes should be recorded to evaluate potential concentration sensitivity to volume variation between sampling events.
- Where it is deemed impractical to routinely remove at least 1 SV using low flow rates, justification should be demonstrated by an initial validation in which samples are taken after removal of at least

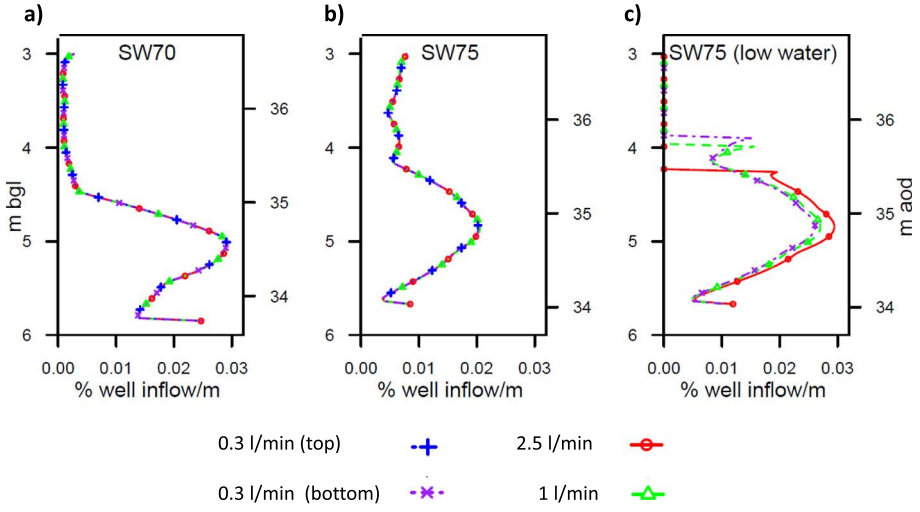

Fig. 11. Monitoring well screen inflows per m as a function of pumping rate with rest water level within the screen interval (pumping rates and pump intake locations are given in Table 2).

1 SV, but ideally up to 3 SV.

- Whilst zero/minimal-purge methods were not used in this study, their deployment in DNAPL source zones should be used cautiously and demonstrated by appropriate individual well validation (e.g., deployment at several depths). The underpinning relationship to purged concentration variation over at least 1 SV should be examined initially and ideally occasionally.

Overall, a key utility of monitoring wells is their potential cost-effective monitoring of contaminant fluxes immediately down-gradient of a DNAPL source zone area. In particular, their proportionately greater sample draw from the more permeable horizons that constitute critical, high-mobility, pathways of contaminant flux to the wider environment. Monitoring wells thereby capture an important, 'representative', fraction of the source mass flux that poses wider risk and may provide a valuable metric of overall bulk source dissolution. With increasing source age, however, availability of complementary higher resolution (e.g., MLS) data is important to help confirm contamination flux contributions from the less permeable horizons expected to prove increasingly important at late time. Indeed, the additional interpretive understanding demonstrated in this study by acquiring higher resolution monitoring data (MLS concentration and K data primarily, supplemented by a detailed tracer test and integrative pumped cell capture of contaminant fluxes) to complement the monitoring well data is significant. Little of the detailed understanding developed may be discerned from the monitoring well installations alone, without reducing to ultra-short screen wells (*c*. 0.3 m being a realistic practical minimum).

In summary, short-screen monitoring wells sampled with validated and informed protocols are shown to have valuable utility in the assessment of DNAPL source zone areas and expected to remain a cost-effective site assessment tool. However, it is essential that complementary high-resolution site data are acquired via the aforementioned technologies to help inform interpretation of the monitoring well data collected. Optimising this data partnership is viewed critical to the cost-effective advancement of the site conceptual model, and for informed remedial design, implementation and performance monitoring.

Acknowledgments

Research fieldwork and modelling was undertaken whilst authors McMillan and Rivett were formerly at the University of Birmingham (School of Geography, Earth and Environmental Sciences) as part of an Open Case Studentship supported by the Natural Environment Research Council (grant NE/H019170/1) and Case Partners Waterra-In-Situ (now In-Situ) and the Environment Agency (for England). The authors are grateful to *Project SABRE* (Source Area BioREmediation) (funded by the UK Bioremediation LINK Programme) for research facilitation, provision of various datasets and technical discussions with the SABRE research consortia members as well as the assistance of the SABRE site owners and their consultants for their generous facilitation of the research. We acknowledge the generosity of ESI Ltd. for providing access to their Groundwater Vistas software.

Appendix A. Supplementary data

Supplementary data to this article can be found online at https://doi.org/10.1016/j.jconhyd.2018.02.001.

References

Adamson, D.T., Chapman, S., Mahler, N., Newell, C., Parker, B., Pitkin, S., Rossi, M., Singletary, M., 2014. Membrane Interface Probe protocol for contaminants in low-permeability zones. Groundwater 52, 550–565. http://dx.doi.org/10.1111/gwat.12085.

Annable, M., Rao, P.S.C., Hatfield, K., Graham, W.D., 1998. Partitioning tracers for measuring residual NAPL: field-scale test results. J. Environ. Eng. 124 (6), 498–503. http://dx.doi.org/10.1061/(ASCE)0733-9372(1998)124:6(498).

Annable, M.D., Hatfield, K., Cho, J., Klammler, H., Parker, B.L., Cherry, J.A., Rao, P.S.C., 2005. Field-scale evaluation of the passive flux meter for simultaneous measurement of groundwater and contaminant fluxes. Environ. Sci. Technol. 39 (18), 7194–7201. http://dx.doi.org/10.1021/es050074g.

Anneser, B., Einsiedl, F., Meckenstock, R.U., Richters, L., Wisotzky, F., Griebler, C., 2008. High-resolution monitoring of biogeochemical gradients in a tar oil-contaminated aquifer. Appl. Geochem. 23, 1715–1730. http://dx.doi.org/10.1016/j.apgeochem.2008.02.003.

Barber, C., Davis, G.B., 1987. Representative sampling of ground water from short-screened boreholes. Ground Water 25 (5), 581–587. http://dx.doi.org/10.1111/j.1745-6584.1987.tb02888.x.

Basu, N.B., Rao, P.S.C., Poyer, I.C., Annable, M.D., Hatfield, K., 2006. Flux-based assessment at a manufacturing site contaminated with trichloroethylene. J. Contam. Hydrol. 86, 105–127. http://dx.doi.org/10.1016/j.jconhyd.2006.02.011.

Basu, N.B., Rao, P.S.C., Poyer, I.C., Nandy, S., Mallavarapu, M., Naidu, R., Davis, G.B., Patterson, B.M., Annable, M.D., Hatfield, K., 2009. Integration of traditional and innovative characterization techniques for flux-based assessment of dense non-aqueous phase liquid (DNAPL) sites. J. Contam. Hydrol. 105 (3–4), 161–172. http://dx.doi.org/10.1016/j.jconhyd.2008.12.005.

Béland-Pelletier, C., Fraser, M., Barker, J., Ptak, T., 2011. Estimating contaminant mass discharge: a field comparison of the multilevel point measurement and the integral pumping investigation approaches and their uncertainties. J. Contam. Hydrol. 122 (1–4), 63–75. http://dx.doi.org/10.1016/j.jconhyd.2010.11.004.

Britt, S.L., Parker, B.L., Cherry, J.A., 2010. A downhole passive sampling system to avoid bias and error from groundwater sample handling. Environ. Sci. Technol. 44 (13), 4917–4923. http://dx.doi.org/10.1021/es100828u.

Britt, S.L., Martin-Hayden, M., Plummer, M.A., 2014. An assessment of aquifer/well flow dynamics: identification of parameters key to passive sampling and application of downhole sensor technologies. In: SERDP Project ER-1704 – Final Report, . https://www.serdp-estcp.org/content/download/32774/319789/file/ER-1704-FR.pdf.

Brooks, M.C., Cha, K.Y., Wood, A.L., Annable, M.D., 2015. Screening-level estimates of mass discharge uncertainty from point measurement methods. J. Contam. Hydrol. 2015 (177–178), 167–182. http://dx.doi.org/10.1016/j.jconhyd.2015.04.002.

Buss, S., Cunningham, C., Ellis, D., Farrar, I., Gerhard, J., Harkness, M., Hart, A., Houlden, L., Lee, M., Wealthall, G., Wilson, R., Zeeb, P., 2010. Project SABRE (Source Area BioRemediation)—an Overview. SABRE Bulletin 1CL. AIRE, London. http://claire.co.uk/index.php?option=com_resource&view=list&category_id=3&Itemid=61.

Cai, Z., Wilson, R.D., Lerner, D.N., 2012. Assessing TCE source bioremediation by geostatistical analysis of a flux fence. Groundwater 50 (6), 908–917. http://dx.doi.org/10.1111/j.1745-6584.2012.00916.x.

Chambers, J.E., Wilkinson, P.B., Wealthall, G.P., Loke, M.H., Dearden, R.A., Wilson, R.D., Ogilvy, R.D., 2010. Hydrogeophysical imaging of deposit heterogeneity and groundwater chemistry changes during DNAPL source zone bioremediation. J. Contam. Hydrol. 118 (1–2), 43–61. http://dx.doi.org/10.1016/j.jconhyd.2010.07.001.

Cherry, J.A., Parker, B.L., Keller, C., 2007. A new depth-discrete multilevel monitoring approach for fractured rock. Groundw. Monit. Remed. 27 (2), 57–70. http://dx.doi.org/10.1111/j.1745-6592.2007.00137.x.

Dearden, R., Chambers, J., Allen, D., Wealthall, G., 2010a. CL:AIRE SABRE Bulletin 2 - Site Investigation Techniques for DNAPL Source and Plume Zone Characterisation. http://www.claire.co.uk/index.php?option=com_phocadownload&view=category&download=194:sabre-bulletin-02&id=13:sabre-bulletins.

Dearden, R., Wealthall, G.P., Chambers, J.E., Rivett, M.O., 2010b. Forced Gradient Conservative Tracer Test in the SABRE Research Cell. British Geological Survey, Commissioned Report CR/09/054 Nottingham, UK.

Dearden, R.A., Noy, D., Lelliott, M., Wilson, R., Wealthall, G., 2013. Release of contaminants from a heterogeneously fractured low permeability unit underlying a DNAPL source zone. J. Contam. Hydrol. 153, 141–155. http://dx.doi.org/10.1016/j.jconhyd.2011.05.006.

Einarson, M.D., Mackay, D.M., 2001. Predicting impacts of groundwater contamination. Environ. Sci. Technol. 35, 66A–73A. http://dx.doi.org/10.1021/es0122647.

FDEP, 2008. Monitoring Well Design and Construction Guidance Manual, Florida Department of Environmental Protection Bureau of Water Facilities Regulation. http://www.dep.state.fl.us/water/groundwater/docs/monitoring-well-manual-formatted-final.pdf.

Fretwell, B.A., Short, R.I., Sutton, J.S., 2006. Guidance on the Design and Installation of Groundwater Quality Monitoring Points, Environment Agency Science Report SC020093. Environment Agency 87 pp. https://www.gov.uk/government/uploads/system/uploads/attachment_data/file/290727/scho0106bkct-e-e.pdf.

Guilbeault, M.A., Parker, B.L., Cherry, J.A., 2005. Mass and flux distributions from DNAPL zones in Sandy aquifers. Ground Water 43 (1), 70–86. http://dx.doi.org/10.1111/j.1745-6584.2005.tb02287.x.

Harbaugh, A.W., Banta, E.R., Hill, M.C., McDonald, M.G., 2000. Modflow-2000, the U.S. Geological Survey modular ground-water model - user guide to modularization concepts and the ground-water flow process, USGS open-file report 00-92. In: US Geological Survey, . http://pubs.usgs.gov/of/2000/0092/report.pdf.

Harkness, M., Fisher, A., Lee, M.D., Mack, E.E., Payne, J.A., Dworatzek, S., Roberts, J., Acheson, C., Herrmann, R., Possolo, A., 2012. Use of statistical tools to evaluate the reductive dechlorination of high levels of TCE in microcosm studies. J. Contam. Hydrol. 131 (1), 100–118. http://dx.doi.org/10.1016/j.jconhyd.2012.01.011.

Harkness, M., Fisher, A., 2013. Use of emulsified vegetable oil to support bioremediation of TCE DNAPL in soil columns. J. Contam. Hydrol. 151, 16–33. http://dx.doi.org/10.1016/j.jconhyd.2013.04.002.

Hutchins, S.R., Acree, S.D., 2000. Ground water sampling bias observed in shallow, conventional wells. Groundw. Monit. Remed. 20 (1), 86–93. http://dx.doi.org/10.

1111/j.1745-6592.2000.tb00255.x.
Hvorslev, M.J., 1951. Time lag and soil permeability in ground-water observations. In: U.C.O.E. Bulletin No. 36, Vicksburg, Mississippi, (50pp (Editor)).
ITRC (Interstate Technology & Regulatory Council), 2006. *Technology Overview of Passive Sampler Technologies.* DSP-4. Washington, D.C.: Interstate Technology & Regulatory Council, Diffusion/Passive Sampler Team. https://clu-in.org/download/char/passsamp/itrc-technology-overview-DSP-4.pdf.
ITRC (Interstate Technology & Regulatory Council), 2007. Protocol for Use of Five Passive Samplers to Sample for a Variety of Contaminants in Groundwater. DSP-5. Washington, D.C.: Interstate Technology & Regulatory Council, Diffusion/Passive Sampler Team. https://www.itrcweb.org/GuidanceDocuments/DSP-5.pdf.
ITRC (Interstate Technology & Regulatory Council), 2015. Integrated DNAPL Site Characterization and Tools Selection (ISC-1). Interstate Technology & Regulatory Council, DNAPL Site Characterization Team, Washington, D.C.. www.itrcweb.org/DNAPL-ISC_tools-selection.
Johnston, C.D., Davis, G.B., Bastow, T.P., Annable, M.D., Trefry, M.G., Furness, A., Geste, Y., Woodbury, R.J., Rao, P.S.C., Rhodes, S., 2013. The use of mass depletion-mass flux reduction relationships during pumping to determine source zone mass of a reactive brominated-solvent DNAPL. J. Contam. Hydrol. 144 (1), 122–137. http://dx.doi.org/10.1016/j.jconhyd.2012.11.005.
Kao, C.M., Wang, Y.S., 2001. Field investigation of the natural attenuation and intrinsic biodegradation rates at an underground storage tank site. Environ. Geol. 40, 622–631. http://dx.doi.org/10.1007/s002540000226.
King, M.W.G., Barker, J.F., Devlin, J.F., Butler, B.J., 1999. Migration and natural fate of a coal tar creosote plume; 2, Mass balance and biodegradation indicators; transport and fate of coal-tar compounds in the subsurface. J. Contam. Hydrol. 39, 281–307. http://dx.doi.org/10.1016/S0169-7722(99)00048-0.
Kram, M.L., Keller, A.A., Rossabi, J., Everett, L.G., 2001. DNAPL characterization methods and approaches, part 1: performance comparisons. Groundw. Monit. Remed. 21, 109–123. http://dx.doi.org/10.1111/j.1745-6592.2001.tb00647.x.
Kueper, B.H., Stroo, H.F., Vogel, C.M., Ward, C.H. (Eds.), 2014. Chlorinated Solvent Source Zone Remediation. Springer, New York (ISBN 978-1-4614-6922-3. SERDP-ESTCP Environmental Remediation Technology, vol. 7, 713 pp).
Lelliot, M.R., Cave, M.R., Wealthall, G.P., 2008. A structured approach to the measurement of uncertainty in 3D geological models. Q. J. Eng. Geol. Hydrogeol. 42 (1), 95–105. http://dx.doi.org/10.1144/1470-9236/07-081.
Li, K.B., Goovaerts, P., Abriola, L.M., 2007. A geostatistical approach for quantification of contaminant mass discharge uncertainty using multilevel sampler measurements. Water Resour. Res. 43 (6). http://dx.doi.org/10.1029/2006WR005427.
Martin-Hayden, J.M., 2000. Sample concentration response to laminar wellbore flow: implications to ground water data variability. Ground Water 89 (1), 12–19. http://dx.doi.org/10.1111/j.1745-6584.2000.tb00197.x.
Martin-Hayden, J.M., Britt, S.L., 2006. Revealing the black box of groundwater sampling: effects of well bore flow and mixing during purging. In: *North American Field Conference and Exposition*, Tampa Florida, January 2006.
Martin-Hayden, J.M., Plummer, M., Britt, S.L., 2014. Controls of wellbore flow regimes on pump effluent composition. Ground Water 52 (1), 96–104. http://dx.doi.org/10.1111/gwat.12036.
McDonald, J.P., Smith, R.M., 2009. Concentration profiles in screened wells under static and pumped conditions. Groundw. Monit. Remed. 29 (2), 78–86. http://dx.doi.org/10.1111/j.1745-6592.2009.01232.x.
McHugh, T.E., Kulkarni, P.R., Beckley, L.M., Newell, C.J., Zumbro, M., 2016. Negative bias and increased variability in VOC concentrations using the HydraSleeve in monitoring wells. Groundw. Monit. R 36, 79–87. http://dx.doi.org/10.1111/gwmr.12141.
McMillan, L.A., Rivett, M.O., Tellam, J.H., Dumble, P., Sharp, H., 2014. Influence of vertical flows in wells on groundwater sampling. J. Contam. Hydrol. 169, 50–61. http://dx.doi.org/10.1016/j.jconhyd.2014.05.005.
Metcalf, M.J., Robbins, G.A., 2007. Comparison of water quality profiles from shallow monitoring wells and adjacent multilevel samplers. Groundw. Monit. Remed. 27 (1), 84–91. http://dx.doi.org/10.1111/j.1745-6592.2006.00126.x.
Pankow, J.F., Cherry, J.A., 1996. Dense Chlorinated Solvents and Other DNAPLs in Groundwater: History, Behavior, and Remediation. Waterloo Press, Portland, OR.
Parker, B.L., Cherry, J.A., Chapman, S.W., Guilbeault, M.A., 2003. Review and analysis of chlorinated solvent dense nonaqueous phase liquid distributions in five Sandy aquifers. Vadose Zone J. 2, 116–137. http://dx.doi.org/10.2136/vzj2003.1160. http://web.cecs.pdx.edu/~gjohnson/Parker%20et%20al%2003.pdf.
Parsons, 2005. Results Report for the Demonstration of No-purge Groundwater Sampling Devices at Former McClellan Air Force Base. Consultant's report to U.S. Army Corps of Engineers (Omaha District), the Air Force Center for Environmental Excellence, and the Air Force Real Property Agency, California 83 pp. https://www.itrcweb.org/Documents/McClellan%20Rpt_Oct2005.pdf.
Pollock, D.W., 1994. User's Guide for MODPATH/MODPATH-PLOT, Version 3: A particle tracking post-Processing Package for MODFLOW, the U.S. Geological Survey finite-Difference Ground-water Flow Model, USGS Open-File Report 94-464. U.S. Geological Survey, Reston, Virginia. http://water.usgs.gov/nrp/gwsoftware/modpath5/ofr94464.pdf.
Puls, R.W., Barcelona, M.J., 1996. Low-flow (Minimal Drawdown) Groundwater Sampling Procedures. EPA/540/S-95/504.
Puls, R.W., Paul, C.J., 1997. Multi-layer sampling in conventional monitoring wells for improved estimation of vertical contaminant distributions and mass. J. Contam. Hydrol. 25 (1–2), 85–111. http://dx.doi.org/10.1016/S0169-7722(96)00026-5.
Reilly, T.E., LeBlanc, D.R., 1998. Experimental evaluation of factors affecting temporal variability of water samples obtained from long-screened wells. Ground Water 36 (4), 270–276. http://dx.doi.org/10.1111/j.1745-6584.1998.tb02830.x.
Rivett, M.O., Allen-King, R.M., 2003. A controlled field experiment on groundwater contamination by a multicomponent DNAPL: dissolved-plume retardation. J. Contam. Hydrol. 66, 117–146. http://dx.doi.org/10.1016/S0169-7722(03)00006-8.
Rivett, M.O., Feenstra, S., 2005. Dissolution of an emplaced source of DNAPL in a natural aquifer setting. Environ. Sci. Technol. 39 (2), 447–455. http://dx.doi.org/10.1021/es040016f.
Rivett, M.O., Dearden, R.A., Wealthall, G.P., 2014. Architecture, persistence and dissolution of a 20 to 45 year old trichloroethene DNAPL source zone. J. Contam. Hydrol. 170, 95–115. http://dx.doi.org/10.1016/j.jconhyd.2014.09.008.
Robin, M.J.L., Gillham, R.W., 1987. Field evaluation of well purging procedures. Groundw. Monit. Remed. 7 (4), 85–93. http://dx.doi.org/10.1111/j.1745-6592.1987.tb00967.x.
Robinson, C., Barry, D.A., McCarty, P.L., Gerhard, J.I., Kouznetsova, I., 2009. pH control for enhanced reductive bioremediation of chlorinated solvent source zones. Sci. Tot. Environ. 407 (16), 4560–4573. http://dx.doi.org/10.1016/j.scitotenv.2009.03.029.
Sukop, M.C., 2000. Estimation of vertical concentration profiles from existing wells. Ground Water 38 (6), 836–841. http://dx.doi.org/10.1111/j.1745-6584.2000.tb00681.x.
US EPA, 1992. Estimating Potential for Occurrence of DNAPL at Superfund Sites, Publication 9355.4-07FS. US Environmental Protection Agency Office of Solid Waste and Emergency Response, Washington DC. http://www.epa.gov/superfund/health/conmedia/gwdocs/pdfs/estdnapl.pdf.
US EPA, 2010. Low Stress (Low Flow) Purging and Sampling Procedure for the Collection of Groundwater Samples From Monitoring Wells, EPASOP-GW001. http://www.epa.gov/region1/lab/qa/pdfs/EQASOP-GW001.pdf.
US EPA, 2013. Groundwater sampling: operating procedure. Region 4 US EPA. Science and Ecosystem Support Division, Athens, Georgia (SESDPROC-301-R3).
US EPA, 2017. Low Stress (Low Flow) Purging and Sampling Procedure for the Collection of Groundwater Samples From Monitoring Wells (Revision Number 4), EPASOP-GW001. https://www.epa.gov/quality/low-stress-low-flow-purging-and-sampling-procedure-collection-groundwater-samples-monitoring.
Varljen, M.D., Barcelona, M.J., Obereiner, J., Kaminski, D., 2006. Numerical simulations to assess the monitoring zone achieved during low-flow purging and sampling. Groundw. Monit. Remed. 26 (1), 44–52. http://dx.doi.org/10.1111/j.1745-6592.2006.00029.x.
Vroblesky, D.A., 2001. User's guide for polyethylene-based passive diffusion bag samplers to obtain volatile organic compound concentrations in wells. In: USGS Report 01-4061, Columbia, South Carolina.
Vroblesky, D.A., Casey, C.C., Lowery, M.A., 2006. Influence of in-well convection on well sampling. In: U.S. Geological Survey Scientific Investigations Report 2006–5247, . https://pubs.usgs.gov/sir/2006/5247/sir20065247.pdf.
Wilson, R., Cai, Z., 2010. CL:AIRE SABRE Bulletin 6 - Source Area DNAPL Bioremediation: Performance Monitoring and Assessment. http://www.claire.co.uk/index.php?option=com_phocadownload&view=category&download=310:sabre-bulletin-06&id=13:sabre-bulletins.
Zeeb, P., Houlden, L., 2010. CL:AIRE SABRE Bulletin 5 - Overview of the SABRE Field Tests. http://claire.co.uk/index.php?option=com_resource&view=list&category_id=3&Itemid=61.
Zheng, C., Wang, P., 1999. MT3DMS A Modular three-dimensional Multispecies Transport Model, Contract Report SERDP-99-1. U.S. Army Corps of Engineers. http://www.dtic.mil/cgi-bin/GetTRDoc?Location=U2&doc=GetTRDoc.pdf&AD=ADA373474.